Changes in $PM_{2.5}$ Peat Combustion Source Profiles with Atmospheric Aging in an Oxidation Flow Reactor

Judith C. Chow[1,2*], Junji Cao[2,3], L.-W. Antony Chen[4], Xiaoliang Wang[1], Qiyuan Wang[2,3], Jie Tian[2,3], Steven Sai Hang Ho[1,5], Adam C. Watts[1], Tessa B. Carlson[1], Steven D. Kohl[1], John G. Watson[1,2]

[1]Division of Atmospheric Sciences, Desert Research Institute, Reno, Nevada, USA

[2]Key Laboratory of Aerosol Chemistry and Physics, Institute of Earth Environment, Chinese Academy of Sciences, Xi'an, 710061, China.

[3]CAS Center for Excellence in Quaternary Science and Global Change, Xi'an, 710061, China

[4]Department of Environmental and Occupational Health, University of Nevada, Las Vegas, Nevada, USA

[5]Hong Kong Premium Services and Research Laboratory, Hong Kong, China

Revised and resubmitted to

Atmospheric Measurement Techniques Discussion

Date

19 August 2019

[*]Corresponding Author: judith.chow@dri.edu

Abstract

Smoke from laboratory chamber burning of peat fuels from Russia, Siberia, U.S.A. (Alaska and Florida), and Malaysia representing boreal, temperate, subtropical, and tropical regions was sampled before and after passing through a potential aerosol mass-oxidation flow reactor (PAM-OFR) to simulate intermediate-aged (~2 days) and well-aged (~7 days) source profiles. Species abundances in $PM_{2.5}$ between aged and fresh profiles varied by several orders of magnitude with two distinguishable clusters, centered around 0.1% for reactive and ionic species and centered around 10 % for carbon.

Organic carbon (OC) accounted for 58–85 % of $PM_{2.5}$ mass in fresh profiles with low EC abundances (0.67–4.4 %). OC abundances decreased by 20–33 % for well-aged profiles, with reductions of 3–14 % for the volatile OC fractions (e.g., OC1 and OC2, thermally evolved at 140 and 280 °C). Ratios of organic matter (OM) to OC abundances increased by 12–19 % from intermediate- to well-aged smoke. Ammonia (NH_3) to $PM_{2.5}$ ratios decreased after intermediate aging.

Well-aged NH_4^+ and NO_3^- abundances increased to 7–8 % of $PM_{2.5}$ mass, associated with decreases in NH_3, low temperature OC, and levoglucosan abundances for Siberia, Alaska, and Everglades (Florida) peats. Elevated levoglucosan was found for Russian peats, accounting for 35–39 % and 20–25 % of $PM_{2.5}$ mass for fresh and aged profiles, respectively. The water-soluble organic carbon (WSOC) fractions of $PM_{2.5}$ were over two-fold higher in fresh Russian (37.0 ± 2.7 %) than in Malaysian (14.6 ± 0.9 %) peats. While Russian peat OC emissions were largely water-soluble, Malaysian peat emissions were mostly water-insoluble, with WSOC/OC ratios of 0.59–0.71 and 0.18–0.40, respectively.

This study shows significant differences between fresh and aged peat combustion profiles among the four biomes that can be used to establish speciated emission inventories for atmospheric modeling and receptor model source apportionment. A sufficient aging time (~one week) is needed to allow gas-to-particle partitioning of semi-volatilized species, gas-phase oxidation, and particle volatilization to achieve representative source profiles for regional-scale source apportionment.

Keywords: fresh and aged source profiles, atmospheric aging, organic mass, organic carbon, levoglucosan, oxidation flow reactor (OFR)

1 Introduction

Receptor-oriented source-apportionment models have played a major role in establishing the weight of evidence (U.S.EPA, 2007) for pollution control decisions. These models, particularly the different solutions (Watson et al., 2016) to the Chemical Mass Balance (CMB) equations (Hidy and Friedlander, 1971), rely on patterns of chemical abundances in different source types that can be separated from each other when superimposed in ambient samples of volatile organic compounds (VOC) and suspended particulate matter (PM). These patterns, termed "source profiles," have been measured in diluted exhaust emissions and resuspended mineral dusts for a variety of representative emitters. Many of these source profiles are compiled in country-specific source profile data bases (Cao, 2018; CARB, 2019; Liu et al., 2017; Mo et al., 2016; Pernigotti et al., 2016; U.S.EPA, 2019) and have been widely used for source apportionment and speciated emission inventories.

Chemical profiles measured at the source have been sufficient to identify and quantify nearby, and reasonably fresh, source contributions. These source types include gasoline- and diesel-engine exhaust, biomass burning, cooking, industrial processes, and fugitive dust. Ambient VOC and PM concentrations have been reduced as a result of control measures applied to these sources, and additional reductions have been implemented for toxic materials such as lead, nickel, vanadium, arsenic, diesel particulate matter, and several organic compounds. As these fresh emission contributions in neighborhood- and urban-scale environments (Chow et al., 2002) decrease, regional-scale contributions that may have aged for intermediate (~2 days) or long (~7 days) periods prior to arrival at a receptor gain in importance. These profiles experience augmentation and depletion of chemical abundances owing to photochemical reactions among their gases and particles, as well as interactions upon mixing with other source emissions.

Peatland fires produce long-lasting thick smoke that leads to adverse atmospheric, climate, ecological, and health impacts. Smoke from Indonesian and Malaysian peatlands is a major concern in the countries of southeast Asia (Wiggins et al., 2018) and elsewhere; it is transported over long distances. Aged peat smoke profiles are likely to differ from fresh emissions, as well as among the different types of peat in other parts of the world.

Ground-based, aircraft, shipboard, and laboratory peat combustion experiments have been carried out to better represent global peat fire emissions and estimate their environmental impacts (e.g., Akagi et al., 2011; Iinuma et al., 2007; Nara et al., 2017; Stockwell et al., 2014; 2016). Most peat fire studies report emission factors (EFs) for pyrogenic gases (e.g., methane, carbon monoxide, and carbon dioxide) and fine particle ($PM_{2.5}$, particles with aerodynamic diameter <2.5 microns) mass, with a few studies reporting EFs for organic and elemental carbon (OC and EC) (Hu et al., 2018).

Despite this lack of peat-specific fresh and aged source profiles, results have been published for source apportionment in Indonesia (See et al., 2007), Malaysia (Fujii et al., 2017), Singapore (Budisulistiorini et al., 2018), and Ireland (Dall'Osto et al., 2013; Kourtchev et al., 2011; Lin et al., 2019). These have involved sampling under near-source and far from-source dominated environments, such as the 2015 Indonesia burning episode to determine changes in thermally-derived carbon fractions with aging (Tham et al., 2019), and inference of aged peat-burning profiles from positive matrix factorization (PMF) application to chemically-speciated ambient PM samples (Fujii et al., 2017). Budisulistiorini et al. (2018) observe that "…atmospheric processing of aerosol particles in haze from Indonesian wildfires has scarcely been investigated. This lack of study inhibits a detailed treatment of atmospheric processes in the models, including aerosol aging and secondary aerosol formation."

Changes in source profiles have been demonstrated in large smog chambers (Pratap et al., 2019), wherein gas/particle mixtures are illuminated with ultraviolet (UV) light for several hours and their end products are measured. Such chambers are specially constructed and limited to laboratory testing. A more recent method for simulating such aging is the oxidation flow reactor (OFR), based on the early studies of Kang et al. (2007), revised and improved by several researchers (e.g., Jimenez, 2018; Lambe et al., 2011), and commercially available from Aerodyne (2019a, b). Although the Aerodyne potential aerosol mass (PAM)-OFR has many limitations, as explained in the supplemental material (Section S.1), it is a practical method for understanding how profiles might change with different degrees of atmospheric aging. A growing users group (PAMWiki, 2019) provides increasing knowledge of its characteristics and operations.

Laboratory peat combustion EFs for gaseous carbon and nitrogen species corresponding with the profiles described here, as well as $PM_{2.5}$ mass and major chemical species (e.g., carbon and ions), are reported by Watson et al. (2019). The $PM_{2.5}$ speciated source profiles derive from six peat fuels collected from Odintsovo, Russia; Pskov, Siberia; Northern Alaska and Florida, U.S.A.; and Borneo, Malaysia; representing boreal, temperate, subtropical, and tropical climate regions. Comparisons between fresh (diluted and unaged) and aged (represent intermediate-aged

[~2 days] and well-aged [~7 days] laboratory simulated oxidation with an OFR) $PM_{2.5}$ speciated profiles are made to highlight chemical abundance changes with photochemical aging. The objectives of this study are to: 1) evaluate similarities and differences among the peat source profiles from four biomes; 2) examine the extent of gas-to-particle oxidation and volatilization between 2- and 7-days of simulated atmospheric aging; and 3) characterize carbon and nitrogen properties in peat combustion emissions.

2 Experiment

The supplemental material describes sampling configuration shown in Fig. S1 and OFR operation. Briefly, peat smoke generated in a laboratory combustion chamber (Tian et al., 2015) was diluted with clean air (by factors of three to five) to allow for nucleation and condensation at ambient temperatures (Watson et al., 2012). These diluted emissions were then passed through an unmodified Aerodyne PAM-OFR in the OFR185 mode without ozone (O_3) injection. Hydroxyl radical (OH) production as a function of UV lamp voltage was estimated by inference from sulfur dioxide (SO_2) decay using well-established rate constants. UV lamps were operated at 2 and 3.5 volts with a flow rate of 10 L min^{-1} and a plug-flow residence time of ~80 s in the 13.3 L anodine-coated reactor, which translates to OH exposures (OH_{exp}) of ~2.6 x 10^{11} and ~8.8 x 10^{11} molecules-sec cm^{-3} at 2 volts and 3.5 volts, respectively.

Transport times between source and receptor of 1 to 10 days are typical of peat burning plumes, and the two OH_{exp} estimates were selected to examine intermediate (~2 days) and long-term (~7 days) atmospheric aging. Other emissions aging experiments (e.g., Bhattarai et al., 2018) cite Mao et al. (2009) for a 24-hour average atmospheric OH concentration (OH_{atm}) of $1.5x10^6$ molecules cm^{-3}. This number appears nowhere in the text of Mao et al. (2009), but it corresponds to the ground-level median value in Mao's Figure 8 plot of OH vs. altitude for Asian outflows over the Pacific Ocean. The individual measurements in the plot range from OH_{atm} near-zero to $5.3x10^6$ molecules cm^{-3}. Altshuller (1989) concluded that "The literature contains reports of atmospheric OH radical concentrations measured during daylight hours ranging from 10^5 molecule cm^{-3} to over 10^8 molecule cm^{-3}, but almost all of the values reported are below $5x10^7$ molecules cm^{-3}." Stone et al. (2012) report atmospheric values ranging from $1.1x10^5$ molecules cm^{-3} in polar environments to $1.5x10^7$ molecules cm^{-3} in a vegetated forest. Uncertainties in OH_{exp} within the OFR are, therefore, not the controlling uncertainty in estimating profile aging times. Added to this uncertainty are reactions among emission constituents that are not embodied in the OFR185 mode that tend to suppress OH_{exp} with respect to that estimated by the SO_2 calibration (Li et al., 2015; Peng et al., 2015; Peng et al., 2016; Peng and Jimenez, 2017; Peng et al., 2018). The "OFR Exposure Estimator" available from the PAMWiki (2019) intends to estimate this OH_{exp}, but detailed VOC from these experiments are insufficient to apply it. The nominal 2- and 7-day aging times determined by dividing OH_{exp} by Mao's $1.5x10^6$ molecules cm^{-3} are subject to these uncertainties, which may increase or decrease the aging time estimates. However, these uncertainties, along with other uncertainties related to peat sample selection, moisture content, and laboratory burning conditions do not negate the value of the measurements reported here. There are distinct differences in the fresh, intermediate-aged, and well-aged profiles that address the concerns expressed by Budisulistiorini et al. (2018).

Forty smoldering-dominated peat combustion tests were conducted that included three to six tests for each type of peat fuel (Table S1). The following analysis uses time-integrated (~40–60 minutes) gaseous and $PM_{2.5}$ filter pack samples collected upstream and downstream of the OFR, representing fresh and aged peat combustion emissions, respectively.

2.1 $PM_{2.5}$ mass and chemical analyses

Measured chemical abundances included $PM_{2.5}$ precursor gases (i.e., nitric acid [HNO_3] and ammonia [NH_3]) as well as $PM_{2.5}$ mass and major components (e.g., elements, ions, and carbon). Water-soluble organic carbon (WSOC), carbohydrates, and organic acids that are commonly used as markers in source apportionment for biomass burning were also quantified (Chow and Watson, 2013; Watson et al., 2016).

The filter pack sampling configurations for the four upstream and two downstream channels along with filter types and analytical instrument specifications are shown in Fig. 1. Multiple sampling channels accommodate different filter substrates that allow for comprehensive chemical speciation. Additional upstream Teflon-membrane and quartz-fiber filters were taken for more specific nitrogen and organic compound analyses that are not reported here. The limited flow through the OFR precludes additional downstream sampling.

Teflon-membrane filters (i.e., channels one and five in Fig. 1) were submitted for: 1) gravimetric analysis by microbalance with ±1 μg sensitivity before and after sampling to acquire $PM_{2.5}$ mass concentrations (Watson et al., 2017); 2) filter light reflectance and transmittance by ultraviolet/visible (UV/Vis) spectrometer (200–900 nm) equipped with an integrating sphere that measures transmitted/reflected light at 1 nm interval (Johnson, 2015); 3) 51 elements (i.e., sodium

[Na] to uranium [U]) by energy-dispersive x-ray fluorescence (XRF) analysis (Watson et al., 1999); and 4) organic functional groups by Fourier Transform Infrared (FTIR) spectrometry. Results from UV/Vis and FTIR spectrometry will be reported elsewhere.

Half of the quartz-fiber filter (i.e., channels two and six) was analyzed for: 1) four anions (i.e., chloride [Cl^-], nitrite [NO_2^-], nitrate [NO_3^-], and sulfate [$SO_4^{=}$]), three cations (i.e., water-soluble sodium [Na^+], potassium [K^+], and ammonium [NH_4^+]), and nine organic acids (including four mono- and five di-carboxylic acids) by ion chromatography (IC) with a conductivity detector (CD) (Chow and Watson, 2017); 2) 17 carbohydrates including levoglucosan and its isomers by IC with a pulsed amperometric detector (PAD); and 3) WSOC by combustion and non-dispersive infrared (NDIR) detection. A portion (0.5 cm^2) of the other half quartz-fiber filter was analyzed for OC, EC, and brown carbon (BrC) by the IMPROVE_A multiwavelength thermal/optical reflectance/transmittance method (Chen et al., 2015; Chow et al., 2007; 2015b); the IMPROVE_A protocol (Chow et al., 2007) reports eight operationally defined thermal fractions (i.e., OC1 to OC4 evolved at 140, 280, 480, and 580 °C in helium atmosphere; EC1 to EC3 evolved at 580, 740, and 840 °C in helium/oxygen atmosphere; and pyrolyzed carbon [OP]) that further characterize carbon properties under different combustion and aging conditions. Citric acid and sodium chloride impregnated cellulose-fiber filters placed behind the Teflon-membrane and quartz-fiber filters, respectively, acquired NH_3 as NH_4^+ and HNO_3 as volatilized nitrate, respectively, with analysis by IC-CD.

Detailed chemical analyses along with quality assurance/quality control (QA/QC) measures are documented in Chow and Watson (2013). For each analysis, a minimum of 10 % of the samples were submitted for replicate analysis to estimate precisions. Precisions associated with each concentration were calculated based on error propagation (Bevington, 1969) of the analytical and sampling volume precisions (Watson et al., 2001).

2.2 $PM_{2.5}$ source profiles

Concentrations of two gases (i.e., NH_3 and HNO_3) and 125 chemical species acquired from each sample pair (fresh vs. aged) were normalized by the $PM_{2.5}$ gravimetric mass to obtain source profiles with species-specific fractional abundances. The following analyses are based on the average of 24 paired profiles (shown in Table 1), grouped by upstream (fresh) and downstream (aged) samples for 2- and 7-day aging (i.e., denoted as Fresh 2 vs. Aged 2 and Fresh 7 vs. Aged 7) for each of the six peats with 25 % fuel moisture. Composite profiles are calculated based on the average of individual abundances and the standard deviation of the average within each group (Chow et al., 2002). Although the standard deviation is termed the source profile abundance uncertainty, it is really an estimate of the profile variability for the same fuels and burning conditions, which exceeds the propagated measurement precision.

To assess changes with fuel moisture content, tests of three sets of Putnam (FL1) peats at 60 % fuel moisture were conducted with resulting profiles shown in Table S2. A few samples were voided due to filter damage or sampling abnormality, which produced five unpaired (either fresh or aged) individual profiles (Table S3). These profiles are reported as they might be useful for future source apportionment studies.

2.3 Equivalence measures

The Student *t*-test is commonly used to estimate the statistical significance of differences between chemical abundances. Two additional measures are used to determine the similarities and differences between profiles: 1) the correlation coefficient (r) between the source profile abundances (F_{ij}, the fraction of species i in peat j) divided by the source profile variabilities (σ_{ij}) that quantifies the strength of association between profiles; and 2) the distribution of weighted differences (residual [R]/uncertainty [U] = $[F_{i1} - F_{i2}]/[\sigma^2_{i1} + \sigma^2_{i2}]^{0.5}$) for < 1σ, 1σ-2σ, 2σ-3σ, and >3σ. The percent distribution of R/U ratios is used to understand how many of the chemical species differ by multiples of the uncertainty of the difference. These measures are also used in the effective variance-chemical mass balance (EV-CMB) receptor model solution that uses the variance (r^2) and the R/U ratio to quantify agreement between measured receptor concentrations and those produced by the source profiles and source contribution estimates (Watson, 2004).

3 Results and discussion

3.1 Similarities and differences among peat profiles

The equivalence measures are used to provide guidance in compositing and comparing the 40 sets of fresh vs. aged profiles. The first comparison is made between two Florida samples from locations separated by ~485 km (i.e., Putnam County Lakebed [FL1] and Everglades National Park [FL2]), representing different geological areas and land uses. Panel A of Table S4 shows that the two profiles yield high correlations (r >0.994), but are statistically different (P <0.002); with over 93 % of the chemical abundance differences within ±3σ. However, when combining both fresh Florida profiles (i.e., all Fresh 2 vs. all Fresh 7 in Panel B), statistical differences are not found, with over 98 % of abundance differences within ± 1σ and P >0.5. Notice that statistical differences are found between the two fresh Florida profiles (i.e., FL1 Fresh 2 vs. FL2 Fresh 2 and FL1 Fresh 7 vs. FL2 Fresh 7 in Panel A) with few (< 0.81 % and 5.6 %) R/U ratios exceeding 3σ; combining the two Florida profiles may cancel out some of the differences. However, paired comparisons of other combined profiles show statistical differences with low *P*-values (P <0.002). To further demonstrate the differences, these two Florida profiles are classified as Subtropical 1 and Subtropical 2 to compare with other biomes.

Similarities and differences in peat profiles by biome are summarized in Table 2. Comparisons are made for: 1) paired fresh vs. aged profiles (i.e., All Fresh vs. All Aged; Fresh 2 vs. Aged 2; and Fresh 7 vs. Aged 7); 2) different experimental tests (i.e., Fresh 2 vs. Fresh 7); and 3) two aging times (i.e., Aged 2 vs. Aged 7). Equivalence measures show that most of these profiles are highly correlated (r >0.97, mostly >0.99) but statistically different (P <0.05), with a few exceptions.

Group comparisons between fresh and aged samples (Panel A of Table 2) show statistical differences for all but Putnam (FL1) peat (P >0.94). This is consistent with Watson et al (2019) where atmospheric aging (7 days) reduced organic carbon EFs (i.e., EF_{OC}) by ~20 – 33 % for all but Putnam (FL1) peats (EF_{OC} remained within ±0.5 %). As OC is a major component of $PM_{2.5}$, no apparent changes in OC and carbon fractions abundances may dictate the lack of statistical differences between the fresh and aged profiles.

Paired comparisons for 2-day aging (Panel B of Table 2) show no statistical differences between the Fresh 2 vs. Aged 2 Putnam (FL1) and Malaysian profiles (P >0.30 and 0.95), which may be due to the low number of samples (n=2) in the comparison; this results in no statistical differences for combined Putnam (FL1) and Malaysian peat comparison (P >0.62). Similar to the findings of combining both fresh Florida profiles (i.e., all Fresh2 vs. all Fresh 7 in Table S4), the two fresh Alaskan profiles (Fresh 2 vs. Fresh 7 in Panel D of Table 2) do not show statistical differences (P >0.12).

Compositing profiles by averaging each of the measured abundances may disguise some useful information. For receptor model source apportionment, region-specific profiles are most accurate for estimating source contributions.

Student *t*-tests for the gravimetric $PM_{2.5}$ mass concentrations (μg m^{-3}) measured upstream and downstream of the OFR (Table S5) show statistically significant differences (P <0.05) between fresh vs. aged $PM_{2.5}$ (i.e., Fresh 2 vs Aged 2 and Fresh 7 vs Aged 7). Fresh 2 and Fresh 7 $PM_{2.5}$ mass concentrations are similar, as expected from replicate tests for the same conditions. Increases in some species abundances offset decreases on other abundances, resulting in similar $PM_{2.5}$ levels for "all Fresh vs. all Aged" comparison.

3.2 Sum of species to $PM_{2.5}$ mass ratios

The sum of the major PM chemical abundances should be less than unity since oxygen, hydrogen, and liquid water content are not measured (Chow et al., 1994; 1996). As shown in Table S6, the sums of elements, ions, and carbon explain averages of ~70–90 % of $PM_{2.5}$ mass for fresh profiles except for Russian peat (62–64 %). The "sum of species" decreased by an average of 6 % and 11 % after 2- and 7-days, respectively. These differences are consistent with loss of semi-volatile organic compounds (SVOCs) in the low temperature carbon fractions, although they are offset by formation of oxygenated compounds during aging. This is true for all but Putnam (FL1) peat, for which the "sum of species" explains nearly the same fraction of $PM_{2.5}$ for the fresh and aged profiles.

3.3 Comparison between fresh and aged profiles

Fresh and aged chemical abundances are compared in Fig. 2. Species abundances vary by several orders of magnitude but exhibit two distinguishable clusters: centered around 0.1 % for reactive and secondary ionic species (e.g., NH_4^+, NO_3^-, and $SO_4^=$) and centered around 10 % for carbon compounds (e.g., OC fractions and WSOC). While most gaseous $NH_3/PM_{2.5}$ ratios exceed 10 %, $HNO_3/PM_{2.5}$ ratios are well below 1 %. Reactive/ionic species and carbon components are mostly above and below the 1:1 line, respectively, implying particle formation and evaporation after atmospheric aging. Large variabilities are found for individual species as noted by the standard deviations associated with each average.

Figure 3 shows the ratio of averages between aged and fresh profiles with increasing ratios from 2- to 7-day aging. Atmospheric aging increased oxalic acid, NO_3^-, NH_4^+, and $SO_4^=$ abundances (likely due to conversion of nitrogen and sulfur gases [e.g., NH_3, NO, NO_2, and SO_2] to particles), but decreased NH_3, levoglucosan, and low temperature OC1 and OC2 abundances in most cases. Large variations are found among measured species (left panels in Fig. 3) as ratios range several orders of magnitude for mineral and ionic species. Consistent with Fig. 2 where most carbon compounds are close to but below the 1:1 line, the right panels in Fig. 3 show the reduction of carbonaceous abundances with aged/fresh ratios between 0.1 and 1. Higher aged/fresh ratios in low temperature OC1 and OC2 after 7-day aging are consistent with additional volatilization with longer aging time.

Atmospheric aging should not change the abundances of mineral species (e.g., Al, Si, Ca, Ti, and Fe), except to the extent that the $PM_{2.5}$ mass (to which all species are normalized) increases or decreases with aging. Large standard deviations associated with the ratio of averages for mineral species in the left panels of Fig. 3 illustrate variabilities among different combustion tests for the less abundant species.

3.4 Carbon abundances

3.4.1 Organic carbon and thermally-evolved carbon fractions

Total carbon (TC, sum of OC and EC) constitutes the largest fraction of $PM_{2.5}$ (Table 1), accounting for 59–87 % and 43–77 % of the $PM_{2.5}$ mass for the fresh and aged profiles, respectively. OC dominates TC with low EC abundances (0.67–4.4 %), as commonly found in smoldering-dominated biomass combustion (Chakrabarty et al., 2006; Chen et al., 2007). The largest OC fractions are high temperature OC3 (15–30 % of $PM_{2.5}$), consistent with past studies for biomass burning emissions (Chen et al., 2007; Chow et al., 2004).

OC abundances decreased with aging time. As shown in Fig. S2, upstream (Fresh 2 and Fresh 7) OC abundances ranged from 58–85 % and decreased by 4–12 % and 20–33 % after 2- and 7-day aging, respectively. The exception is for Putnam (FL1) peat, where the OC abundances were similar (changed by ~0.5 to 1.5%) between fresh and aged profiles. Part, but not all of this reduction is due to increasing abundances of non-carbon components, particularly nitrogen-containing species that add to $PM_{2.5}$ mass. OC abundance decreases after aging for other profiles may have contributed to the statistical differences found between fresh and aged $PM_{2.5}$ mass (Table S5). With the exception of Putnam (FL1) peat, the additional 7–22% OC degradation from 2- to 7-day aging implies that much of the OC changes require about a week of aging time.

The Student *t*-test for fresh and aged profiles shows statistical differences (P <0.05) for TC, OC, and low temperature OC1 and OC2, but similarities for OC3 and OC4. High temperature OC3 and OC4 contain more polar and/or high molecular-weight organic components (Chen et al., 2007) that are less likely to photochemically degrade. Large fractions of pyrolized carbon (OP of 7–13 %) are also found, indicative of higher molecular-weight compounds that are likely to char (Chow et al., 2001; Chow et al., 2004; Chow et al., 2018).

Reduction in OC abundances after atmospheric aging is attributed mostly to decreases in low temperature OC1 and OC2 abundances in the OFR as shown in the fresh vs. aged ratios of average abundances (Fig. 3). Figure S3a shows reductions in OC1 abundances after 2- and 7-days of atmospheric aging is apparent but at a similar level: ranging from 2–10 % and 3–14 %, respectively. Additional OC1 reductions from 2- to 7-days are most apparent for Russia and Everglades (FL2) peats at the 6–10 % level. Similar reductions are found for OC2 (Fig. S3b): ranging from 3–11 % and 3–12 % after the 2- and 7-days of aging, respectively. Prolonged aging times resulted in additional 4–8 % OC2 reduction for all but Russian and Putnam (FL1) peats. As oxidation of organic compounds with OH radicals is an efficient chemical aging process (Chim et al., 2018), some of the VOCs and SVOCs may have been liberated (Smith et al., 2009).

3.4.2 Organic mass (OM) and OM/OC ratios

Reduction of the “sum of species” and OC abundances from fresh to aged profiles can be offset by the formation of oxygenated organic compounds as the profiles age. Different assumptions have been used to transform OC to organic mass (OM) to account for unmeasured H, O, N, and S in organic compounds (Cao, 2018; Chow et al., 2015a; Riggio et al., 2018). As single multipliers for OC cannot capture changes by oxidation in the OFR, OM is calculated by subtracting mineral components (using the IMPROVE soil formula by Malm et al. (1994)), major ions (i.e., NH_4^+, NO_3^-, and $SO_4^=$), and EC from $PM_{2.5}$ mass to account for unmeasured mass in organic compounds (Chow et al., 2015a; Frank, 2006). This approach assumes that no major chemical species are unmeasured and that the remaining mass consists of H, O, N, and S associated with OC in forming OM.

Table 3 shows that OM/OC ratios ranged from 1.1–1.7 and 1.3–2.2 for fresh and aged profiles, respectively. The lower OM/OC ratios in fresh emissions are consistent with those reported for other types of biomass burning (Chen et al., 2007; Reid et al., 2005). Figure S4 shows a general upward trend in OM/OC ratios after atmospheric aging with additional 14–21 % increases from 2- to 7-days for all but Putnam (FL1) peat. The increase in OM/OC ratios with aging are likely due to an increase in oxygenated organics. The OM/OC ratio of 1.20 ± 0.05 for fresh Borneo, Malaysian peat is consistent with the 1.26 ± 0.04 ratio for fresh peat burning emissions in Central Kalimantan, Indonesia (Jayarathne et al., 2018), both located on the Island of Borneo.

The highest OM/OC ratios are found for Russian peat, ranging 1.6–1.7 for fresh profiles and increasing to 2.1–2.2 for aged profiles, consistent with formation of low vapor pressure oxygenated compounds in the OFR. Watson et al. (2019) report that the Russian peat fuel contains the lowest carbon (44.20 ± 1.01 %) and highest oxygen (38.64 ± 0.78 %) contents among the six peats. The low carbon contents in peat fuel and source profiles are consistent with the lowest "sum of species" found in Russian peat, with 62–64 % and 50–52 % of $PM_{2.5}$ mass for the fresh and aged profiles, respectively. After 7-day aging for Siberian peat, the increasing OM/OC ratios from 1.2 ± 0.14 to 1.5 ± 0.18 are similar to the increase from 1.22 to 1.42 reported by Bhattarai et al. (2018).

3.4.3 Water-soluble organic carbon (WSOC)

WSOC abundances in $PM_{2.5}$ were over two-fold higher in fresh Russian (36–37 %) than Malaysian (15–17 %) peat. The 15–17 % WSOC in $PM_{2.5}$ for fresh Borneo, Malaysian peat (Table 1) is consistent with the 16 ± 11 % from Central Kalimantan, Indonesia peat (Jayarathne et al., 2018). However, the WSOC/$PM_{2.5}$ ratio is not a good indicator of changes in WSOC abundances during atmospheric aging as $PM_{2.5}$ also contains non-water-soluble and non-carbonaceous aerosol. Table S7 shows large variabilities associated with the differences (i.e., aged minus fresh), suggesting that no differences exist within ±3 standard deviations. The only exceptions are for the 7-day Putnam (FL1) peat and 2-day Malaysian peat, where aging resulted in 7–8 % increases of WSOC abundances in $PM_{2.5}$.

As WSOC is part of the OC, the WSOC/OC ratio is a better indicator of atmospheric aging. WSOC/OC ratios (Table 3) vary between fresh (0.18–0.64) and aged (0.31–0.71) profiles. Figure S5 shows a general increase of WSOC/OC ratios from fresh to aged profiles. Longer aging time from 2- to 7-days results in 5–10 % higher WSOC/OC ratios for all but the two Florida peats. OC water-solubility also varies by peat type. Russian peat OC emissions are largely water-soluble, whereas Malaysian peat emissions are mostly water-insoluble, with WSOC/OC ratios of 0.59–0.71 and 0.18–0.40, respectively.

3.4.4 Carbohydrates

Bates et al. (1991) found that peat from Sumatra, Indonesia consisted of 18–46 % carbohydrate (mainly levoglucosan) relative to total carbon based on nuclear magnetic resonance spectroscopy. Levoglucosan and its isomers (mannosan and galactosan) are saccharide derivatives formed from incomplete combustion of cellulose and hemi-cellulose (Kuo et al., 2008;

Louchouarn et al., 2009) and have been used as markers for biomass burning in receptor model source apportionment (Bates et al., 1991; Watson et al., 2016). These carbohydrate-derived pyrolysis products undergo heterogeneous oxidation when exposed to OH radicals in the OFR (Hennigan et al., 2010; Kessler et al., 2010).

Only five of the 17 carbohydrates (Table 1) were detected, with noticeable variations (e.g., >2 orders of magnitude) in levoglucosan for boreal and temperate peats. Levoglucosan abundances account for 35–39 % and 20–25 % of $PM_{2.5}$ mass for fresh and aged Russian profiles, respectively. On a carbon basis, Table 3 shows that levoglucosan-carbon (with an OM/OC ratio of 2.25) accounts for 42–48 % and 30–35 % of WSOC and 27–28 % and 21–24 % of OC for fresh and aged Russian profiles, respectively. These levels are less than the 96 ± 3.8 % levoglucosan or ~42.7 % of levoglucosan-carbon in OC reported for German and Indonesian peats (Iinuma et al., 2007). Elevated levoglucosan is also found for Siberian and Alaskan peats, ranging from 4–18 % in $PM_{2.5}$. However, the levoglucosan abundances are low (1–4 %) for the subtropical and tropical peats. Aging time of 7 days resulted in an additional 1–4 % levoglucosan degradation relative to 2 days with the exception of an additional 9 % reduction for Russian peat.

The extent of levoglucosan degradation depends on organic aerosol composition, OH exposure in the OFR, and vapor-wall losses (Bertrand et al., 2018a; 2018b; Pratap et al., 2019). Figure 4 shows the presence of levoglucosan-carbon for the Russian and Alaskan peats after 2- and 7-day aging, at the levels of 8–11 % and 2–9 %, respectively, in line with a chemical lifetime longer than 2 days. This is consistent with the estimated 1.2–3.9 days of levoglucosan lifetimes under different environments reported by Lai et al. (2014). However, other studies (Hennigan et al., 2010; May et al., 2012; Pratap et al., 2019) found that levoglucosan experiences rapid gas-phase oxidation, resulting in ~1–2 day lifetimes at ambient temperatures.

Among the carbohydrates, Jayarathne et al. (2018) reported 4.6 ± 4.0 % of levoglucosan in OC for fresh Indonesia peat. Converting to levoglucosan-carbon in Jayarathne et al. (2018) yields a fraction of 2 %, consistent with findings for Malaysian peat (1.4–2.4 %) in this study.

While the presence of levoglucosan in peat smoke is apparent, its isomer, galactosan was not detectable. Mannosan is detectable in cold climate peats with 1–5 % of $PM_{2.5}$ for the Russian and Alaskan peats and up to 1.3 % for Siberian peat. Apparent degradations from 3.9 to 2.5 % and from 5.0 to 2.1 % in mannosan abundances are found for Russian peat (Table 1) after 2- and 7-days, respectively. A 2- to 3-fold reduction in mannosan is also shown after 7 days aging for the

Siberian and Alaskan peats. Similar observations apply to glycerol in Russian peat, ranging 1.9–3.5 % and 1.3–1.7 % of $PM_{2.5}$ for fresh and aged profiles, respectively. Other detectable carbohydrates are galactose and mannitol, typically present at one hundredth of one percent of the levoglucosan abundance.

3.4.5 Organic acids

Organic acids have been associated with many anthropogenic sources, including engine exhaust, biomass burning, meat cooking, bioaerosol, and biogenic emissions. Past studies show the presence of low molecular-weight dicarboxylic acids in biomass burning emissions (e.g., Falkovich et al., 2005; Veres et al., 2010).

Only four of the ten measured organic acids (Table 1) (i.e., formic acid, acetic acid, oxalic acid, and propionic acid) were detectable with variable abundances (<0.02–3.9 %). The largest changes between fresh and aged profiles are found for oxalic acid, ranging from <0.02–0.43 % of $PM_{2.5}$ for fresh profiles, with ~10- to 20-fold increase after 2 days (0.6–1.3 %), and with one to two orders of magnitude increases after 7 days (1.1–3.9 %). With the exception of Putnam (FL1) peat (1.1 ± 0.19 %), oxalic acid accounts for >2.9 % of $PM_{2.5}$ mass after 7 days.

Acetic acid abundances are stable between fresh and aged profiles, mostly in the range of 0.2–0.5 % except for a 6-fold increase from 0.23 ± 0.15 % (Fresh 7) to 1.5 ± 2.0 % (Aged 7) for Siberian peat with large variability among the tests. Formic acid and propionic acid abundances are low (<0.5 and <0.02 %, respectively), but increase with aging. Extending the aging time from 2- to 7-days resulted in a notable increase in organic acid abundances, consistent with the increases in WSOC/OC ratios (Table 3). By biome, the highest abundances for organic acids in $PM_{2.5}$ are found for aged (Aged 7) Siberian peat, with 3.9 ± 1.4 % oxalic acid, 1.5 ± 2.0 % acetic acid, and 0.44 ± 0.28 % formic acid (Table 1).

3.5 Nitrogen species, sulfate, and chloride abundances

Ammonia normalized to $PM_{2.5}$ mass is high for fresh profiles, ranging 17–64 %, except for the low NH_3 content in Russian peat (6–8 %). These abundances are reduced to 3–14 % and 1–7 % after 2- and 7-day aging, respectively. As shown in Fig. 5, most of the NH_3 rapidly diminished after 2 days, with increasing particle-phase NH_4^+ and NO_3^- after 7 days. The highest NH_3 to $PM_{2.5}$ ratios are found for fresh Everglades (FL2) peat profiles (51–64 %), ~2–8 fold higher than other peats. These high and low $NH_3/PM_{2.5}$ ratios are consistent with the nitrogen contents in peat fuel: 3.93 ± 0.08 % for Everglades and 1.50 ± 0.52 % for Russian peats (Watson et al., 2019).

Ionic abundances are typically <0.5 %, especially in fresh profiles. Abundances of NH_4^+ in $PM_{2.5}$ are low (0.0005–0.13 %) for fresh emissions, but increase to 0.05–1.0 % after 2 days and 3.4–6.7 % after 7 days, with the exception of Putnam (FL1) peat (1.01 ± 0.05 % NH_4^+). Extending the aging time from 2- to 7-days results in an additional increase of ~1–7 % NH_4^+ abundances, in contrast to NH_3 that is largely depleted after 2 days.

Figure 5b shows increasing in NO_3^- abundances with aging, 0.04–0.23 % for fresh profiles, increasing to 0.74–2.64 % after 2 days, and to 2.0–8.2 % after 7 days with the exception of Putnam (FL1) peat (1.10 ± 0.18 % NO_3^-). After 7 days, NH_4^+ and NO_3^- account for ~4–7 % and ~8 % of $PM_{2.5}$ mass, respectively, for Siberian, Alaskan, and Everglades (FL2) peats. No specific trend is evident for NO_2^-, mostly <0.002 %, with ~0.2 % for some fresh Siberian and Alaskan peats. The ratio of gaseous HNO_3 to $PM_{2.5}$ is low, in the range of 0.2–0.5 % without much changes between fresh and aged profiles. HNO_3 created through photochemistry is largely neutralized by the abundant NH_3 in the emissions, resulting in the increasing NH_4^+ and NO_3^- to $PM_{2.5}$ in aged profiles.

The reaction of NH_3 with HNO_3 to form ammonium nitrate (NH_4NO_3) is the main pathway for inorganic aerosol formation, owing to low sulfur content in the peat fuels (Watson et al., 2019). $SO_4^=$ abundances are low in fresh profiles (0.13–1.4 %), but they increase 2–3 fold after 2 days aging except for the Alaskan (0.35–0.46 %) and Everglades (FL2) (1.3–1.4 %) profiles. More apparent changes are found for 7 days with the largest increase in $SO_4^=$ from 0.13 to 1.96 % for the Malaysian peats –indicating formation of ammonium sulfate ($[NH_4]_2SO_4$). The ion balance shows more NH_4^+ than needed to completely neutralize NO_3^- and $SO_4^=$ (Chow et al., 1994). Some NH_4^+ may be present as ammonium chloride (NH_4Cl), however, the abundance of chloride (Cl^-) is low (<0.3 %). The large increase in NO_3^- and $SO_4^=$ after 7 days implies that a 2-day aging time is not sufficient to allow the full formation of secondary NH_4NO_3 and $(NH_4)_2SO_4$.

3.6 Mass reconstruction

Mass reconstruction is applied to understand the changes in major chemical composition between the fresh and aged profiles. As shown in Fig. 6, the largest component of $PM_{2.5}$ is OM, accounting for 94–99 % and 80–95 % of $PM_{2.5}$ mass for fresh and aged profiles, respectively. Although the 7-day aging time increased the OM/OC ratios (by 12–19 %), the abundances of OM in $PM_{2.5}$ are reduced (3–18 %). This can be attributed to the combined effects of increased oxygenated organics; SVOC volatilization (Smith et al., 2009); and an increase in ionic species as shown in the average aged/fresh ratios in Fig. 3. Figure 6 shows increases in ionic species (i.e., sum of NH_4^+, NO_3^-, and $SO_4^=$), with low abundances (0.3–1.7 %) in fresh profiles, and increasing 3–16 % after aging. The sum of ionic species accounts for 11–16 % of $PM_{2.5}$ mass for the Siberian, Alaskan, Everglades (FL2), and Malaysian peats after 7 days, mainly due to the increase in NH_4^+ and NO_3^- as shown in Fig. 5.

Elemental abundances are low (<0.0001 %), mostly below the lower quantifiable limits. Table 1 only lists 34 of the 51 elements (Na to U) detected by XRF. Using the IMPROVE soil formula (assuming metal oxides of major mineral species (Malm et al., 1994) yielded 0.07–2.9 % of mineral components. The IMPROVE soil formula has been applied in many other studies (e.g., Chan et al., 1997; Pant et al., 2015; Rogula-Kozlowska et al., 2012) which provides an adequate estimate of geological mineral in reconstructed mass. Since geological minerals are not a major component of $PM_{2.5}$, variations in the assumption regarding metal oxides or multipliers do not contribute to large variations in reconstructed mass (Chow et al., 2015a).

This study indicates that an aging time of ~2 days represents the intermediate-aged source profile, whereas 7 days represents the profile with adequate residence time to complete the atmospheric process.

3.7 Changes in source profiles by fuel moisture content

The effect of fuel moisture content on source profiles is mostly unknown. The 25 % fuel moisture content selected for this study intends to better simulate the conditions of moderate to severe droughts where most peat fires occur. Increasing fuel moisture content from ~25 to 60 % for the three Putnam (FL1) peat fuels yielded 12 % higher EFs for CO_2 (EF_{CO_2}), but 12–20 % lower EFs for CO, NO, NO_2, and $PM_{2.5}$ mass (Watson et al., 2019). Tests of fuel-moisture content on profile changes are available for only 2-day aging. Equivalence measures (Table S8) show statistical differences (P <0.001) between 25 % and 60 % moisture profiles for either fresh or aged profiles with high correlations (r >0.997) and over 93 % of species abundance fall within $\pm 3\sigma$. While OC abundances in $PM_{2.5}$ are comparable for the fresh and aged profiles (70–72 %) for 25 % fuel moisture, a reduction of 18 % OC in $PM_{2.5}$ is found for 60 % fuel moisture (from 82 to 64 %) after aging (Table S2). The higher fuel moisture content also reduced WSOC by 6 % and levoglucosan by 1.3 % with <1 % increases for NH_4^+ and organic acids. After aging, the NH_3 to $PM_{2.5}$ ratios decreased from 28 % to 5 % and from 20 % to 8 % for the 25 % and 60 % fuel moisture, respectively. These results are not conclusive as most measurements are associated with high variabilities.

4 Summary and conclusion

Fresh and aged peat fire emission profiles from laboratory combustion chamber and potential aerosol mass-oxidation flow reactor (PAM-OFR) for six types of peats representing boreal (Odintsovo, Russia and Pskov, Siberia), temperate (Northern Alaska, USA), subtropical (Putnam County Lakebed and Everglades National Park, Florida, USA), and tropical (Borneo, Malaysia) biomes are compared. Analyses are focused on the average of 24 paired profiles grouped by six peats and by fresh vs. aged profiles for 2- and 7-days of simulated atmospheric aging that represent intermediate-aged and well-aged source profiles, respectively.

Equivalence measures show that these profiles are highly correlated (r >0.97, mostly >0.99) but statistically different (P <0.05) between different biomes, suggesting that these profiles should be used independently for receptor model source apportionment studies in different climate regions.

The sum of chemical species (i.e., elements, ions, and carbon) explains an average of ~70–90 % of $PM_{2.5}$ mass for fresh profiles except for Russian peat (62–64 %), confirming that major $PM_{2.5}$ chemical species are measured. Aging times of 2- and 7-days resulted in an average mass depletion of 6 % and 11 %, respectively. These differences are caused by: 1) loss of SVOCs with aging, as indicated by lower abundances of OC1 and OC2 (evolved at 140 and 280 °C) in the aged profiles; and 2) replacement of the lost OC mass with unmeasured oxygen associated with secondary organic aerosol formation in the OFR.

Species abundances in $PM_{2.5}$ between aged and fresh profiles varied by several orders of magnitude but exhibited two distinguishable clusters, with reactive/ionic species (e.g., NH_4^+, $SO_4^=$, oxalic acid, and HNO_3) constituting 0.1–1 % and carbon compounds (e.g., OC, organic carbon fractions [OC1–OC4], and WSOC) constituting >1 % (mostly >10 %) of $PM_{2.5}$ mass. Most $NH_3/PM_{2.5}$ ratios are >10 % whereas $HNO_3/PM_{2.5}$ ratios are <1 %.

Total carbon (TC, sum of OC and EC) is the largest component, accounting for 59–87 % and 43–77 % of the $PM_{2.5}$ mass for the fresh and aged profiles, respectively. With predominant smoldering combustion, the majority of the TC is OC, with low EC abundances (0.67–4.4 %). Further degradation in OC abundances (7–22 %) from 2- to 7-day aging implies an incomplete transformation with short aging time. Different thermal carbon fractions are used to characterize combustion and aging conditions. While most of the OC thermally evolved at high temperatures (OC3 at 480 °C), losses of low temperature OC1 and OC2 are found, indicating a shift of gas-particle partitioning of SVOC to gas-phase, where particle volatilization outweighed gas-to-particle conversion.

Formation of oxygenated compounds is pronounced after aging, with organic mass (OM) to OC ratios increasing by 14–21 % from 2- to 7-day aging. The WSOC abundance in $PM_{2.5}$ varies from 15–17 % and 37–37 % for fresh Malaysian and Russian peats, respectively. While levoglucosan accounts for ~1–4 % of $PM_{2.5}$ mass for fresh subtropical and tropical peats, elevated levels (6–39 %) are found for boreal and temperate peats. Increasing the atmospheric aging time from 2- to 7-days results in additional formation of organic acid and ionic species (e.g., oxalic acid, NO_3^-, NH_4^+, and $SO_4^{=}$), but enhanced losses of NH_3, levoglucosan, and low temperature OC1 and OC2.

Among the four climate regions, Russian peat with the lowest carbon (44 %) and highest oxygen (39 %) content, resulted in ~59–71 % of WSOC in OC along with the highest levoglucosan (20–39 % of $PM_{2.5}$) and lowest $NH_3/PM_{2.5}$ ratios (3–8 %). It also yielded the highest oxygenated compounds after aging with OM/OC ratios of 2.1–2.2. This contrasts with Malaysian peats that are mostly water-insoluble (WSOC/OC of 0.18–0.40) with low oxygenated compounds after aging (OM/OC ratios of 1.2–1.5). Large increases are found for oxalic acid abundances from fresh (<0.02–0.43 %) to 7-day aging (1–4%).

With the exception of Russian peats, fresh profiles contain high $NH_3/PM_{2.5}$ ratios (17–64 %) with low abundances after aging (3–14 % for 2 days and 1–7 % for 7 days). Extending the aging time from 2- to 7-days results in an increase to ~7–8 % NH_4^+ and NO_3^- abundances. Although the week-long aging time increased the OM/OC ratios, abundances of OM in $PM_{2.5}$ were reduced by 3–18 %.

Source profiles can change with aging during transport from source to receptor. This study shows significant differences between fresh and aged peat combustion profiles among the four biomes that can be used to establish speciated emission inventories for air quality modeling. A sufficient aging time (~one week) is needed to allow gas-to-particle partitioning of semi-volatilized species, gas-phase oxidation, and volatilization to achieve representative source profiles for receptor-oriented source apportionment.

5 Author contribution

JCC, JGW, JC, L-WAC, and XW jointly designed the study, performed the data analyses, and prepared the manuscript. ACW collected the peat fuels and provided technical advice. QW, JT, and SSHH carried out the peat combustion experiments. TBC and SDK assembled the database and performed the similarity and difference tests between the fresh and aged profiles.

6 Competing interests

The authors declare that there are no conflicts of interest.

7 Acknowledgements

This research was primarily supported by the National Science Foundation (NSF, AGS1464501) as well as internal funding from both the Desert Research Institute, Reno, NV, USA, and Institute of Earth Environment, Chinese Academy of Sciences, Xian, China.

8 References

Aerodyne: PAM users manual, Aerodyne Research Inc., Billerica, MA, 2019a. https://pamusersmanual.jimdo.com/

Aerodyne: Potential Aerosol Mass (PAM) oxidation flow reactor, Aerodyne Research Inc., Billerica, MA, 2019b. http://www.aerodyne.com/sites/default/files/u17/PAM%20Potential%20Aerosol%20Mass%20Reactor.pdf

Akagi, S. K., Yokelson, R. J., Wiedinmyer, C., Alvarado, M. J., Reid, J. S., Karl, T., Crounse, J. D., and Wennberg, P. O.: Emission factors for open and domestic biomass burning for use in atmospheric models, Atmos. Chem. Phys, 11, 4039-4072, 2011.

Altshuller, A. P.: Ambient air hydroxyl radical concentrations: Measurements and model predictions, J. Air Pollut. Control Assoc., 39, 704-708, 1989.

Bates, A. L., Hatcher, P. G., Lerch, H. E., Cecil, C. B., Neuzil, S. G., and Supardi: Studies of a petified angiosperm log cross-section from Indonesia by nuclear-magnetic resonance spectroscopy and analytical pyrolysis, Organic Geochemistry, 17, 37-45, 1991.

Bertrand, A., Stefenelli, G., Jen, C. N., Pieber, S. M., Bruns, E. A., Ni, H. Y., Temime-Roussel, B., Slowik, J. G., Goldstein, A. H., El Haddad, I., Baltensperger, U., Prevot, A. S. H., Wortham, H., and Marchand, N.: Evolution of the chemical fingerprint of biomass burning organic aerosol during aging, Atmos. Chem. Phys, 18, 7607-7624, 2018a.

Bertrand, A., Stefenelli, G., Pieber, S. M., Bruns, E. A., Temime-Roussel, B., Slowik, J. G., Wortham, H., Prevot, A. S. H., El Haddad, I., and Marchand, N.: Influence of the vapor wall loss on the degradation rate constants in chamber experiments of levoglucosan and other biomass burning markers, Atmos. Chem. Phys, 18, 10915-10930, 2018b.

Bevington, P. R.: Data Reduction and Error Analysis for the Physical Sciences, McGraw Hill, New York, NY, 1969.

Bhattarai, C., Samburova, V., Sengupta, D., Iaukea-Lum, M., Watts, A. C., Moosmuller, H., and Khlystov, A. Y.: Physical and chemical characterization of aerosol in fresh and aged emissions from open combustion of biomass fuels, Aerosol Sci. Technol., 52, 1266-1282, 2018.

Budisulistiorini, S. H., Riva, M., Williams, M., Miyakawa, T., Chen, J., Itoh, M., Surratt, J. D., and Kuwata, M.: Dominant contribution of oxygenated organic aerosol to haze particles from real-time observation in Singapore during an Indonesian wildfire event in 2015, Atmos. Chem. Phys, 18, 16481-16498, 2018.

Cao, J. J.: A brief introduction and progress summary of the $PM_{2.5}$ source profile compilation project in China, Aerosol Science and Engineering, 2, 43-50, 2018.

CARB: Speciation profiles used in ARB modeling, California Air Resources Board, Sacramento, CA, 2019. http://arb.ca.gov/ei/speciate/speciate.htm

Chakrabarty, R. K., Moosmüller, H., Garro, M. A., Arnott, W. P., Walker, J., Susott, R. A., Babbitt, R. E., Wold, C. E., Lincoln, E. N., and Hao, W. M.: Emissions from the laboratory combustion of wildland fuels: Particle morphology and size, J. Geophys. Res. Atmos., 111, D07204, 2006.

Chan, Y. C., Simpson, R. W., McTainsh, G. H., Vowles, P. D., Cohen, D. D., and Bailey, G. M.: Characterisation of chemical species in $PM_{2.5}$ PM_{10} aerosols in Brisbane, Australia, Atmos. Environ., 31, 3773-3785, 1997.

Chen, L.-W. A., Chow, J. C., Wang, X. L., Robles, J. A., Sumlin, B. J., Lowenthal, D. H., Zimmermann, R., and Watson, J. G.: Multi-wavelength optical measurement to enhance thermal/optical analysis for carbonaceous aerosol, Atmos. Meas. Tech., 8, 451-461, 2015.

Chen, L.-W. A., Moosmüller, H., Arnott, W. P., Chow, J. C., Watson, J. G., Susott, R. A., Babbitt, R. E., Wold, C. E., Lincoln, E. N., and Hao, W. M.: Emissions from laboratory combustion of wildland fuels: Emission factors and source profiles, Environ. Sci. Technol., 41, 4317-4325, 2007.

Chim, M. M., Lim, C. Y., Kroll, J. H., and Chan, M. N.: Evolution in the reactivity of citric acid toward heterogeneous oxidation by gas-phase OH radicals, ACS Earth and Space Chemistry, 2, 1323-1329, 2018.

Chow, J. C., Engelbrecht, J. P., Watson, J. G., Wilson, W. E., Frank, N. H., and Zhu, T.: Designing monitoring networks to represent outdoor human exposure, Chemosphere, 49, 961-978, 2002.

Chow, J. C., Fujita, E. M., Watson, J. G., Lu, Z., Lawson, D. R., and Ashbaugh, L. L.: Evaluation of filter-based aerosol measurements during the 1987 Southern California Air Quality Study, Environ. Mon. Assess, 30, 49-80, 1994.

Chow, J. C., Lowenthal, D. H., Chen, L.-W. A., Wang, X. L., and Watson, J. G.: Mass reconstruction methods for $PM_{2.5}$: A review, Air Qual. Atmos. Health, 8, 243-263, 2015a.

Chow, J. C., Riggio, G. M., Wang, X. L., Chen, L.-W. A., and Watson, J. G.: Measuring the organic carbon to organic matter multiplier with thermal/optical carbon mass spectrometer analyses, Aerosol Science and Engineering, 2, 165-172, 2018.

Chow, J. C., Wang, X. L., Sumlin, B. J., Gronstal, S. B., Chen, L.-W. A., Trimble, D. L., Kohl, S. D., Mayorga, S. R., Riggio, G. M., Hurbain, P. R., Johnson, M., Zimmermann, R., and Watson, J. G.: Optical calibration and equivalence of a multiwavelength thermal/optical carbon analyzer, Aerosol Air Qual. Res., 15, 1145-1159, 2015b.

Chow, J. C. and Watson, J. G.: Chemical analyses of particle filter deposits. In: Aerosols Handbook : Measurement, Dosimetry, and Health Effects, Ruzer, L. and Harley, N. H. (Eds.), CRC Press/Taylor & Francis, New York, NY, 2013.

Chow, J. C. and Watson, J. G.: Enhanced ion chromatographic speciation of water-soluble $PM_{2.5}$ to improve aerosol source apportionment, Aerosol Science and Engineering, 1, 7-24, 2017.

Chow, J. C., Watson, J. G., Chen, L.-W. A., Arnott, W. P., Moosmüller, H., and Fung, K. K.: Equivalence of elemental carbon by Thermal/Optical Reflectance and Transmittance with different temperature protocols, Environ. Sci. Technol., 38, 4414-4422, 2004.

Chow, J. C., Watson, J. G., Chen, L.-W. A., Chang, M.-C. O., Robinson, N. F., Trimble, D. L., and Kohl, S. D.: The IMPROVE_A temperature protocol for thermal/optical carbon analysis: Maintaining consistency with a long-term database, J. Air Waste Manage. Assoc., 57, 1014-1023, 2007.

Chow, J. C., Watson, J. G., Crow, D., Lowenthal, D. H., and Merrifield, T. M.: Comparison of IMPROVE and NIOSH carbon measurements, Aerosol Sci. Technol., 34, 23-34, 2001.

Chow, J. C., Watson, J. G., Lu, Z., Lowenthal, D. H., Frazier, C. A., Solomon, P. A., Thuillier, R. H., and Magliano, K. L.: Descriptive analysis of $PM_{2.5}$ and PM_{10} at regionally representative locations during SJVAQS/AUSPEX, Atmos. Environ., 30, 2079-2112, 1996.

Dall'Osto, M., Ovadnevaite, J., Ceburnis, D., Martin, D., Healy, R. M., O'Connor, I. P., Kourtchev, I., Sodeau, J. R., Wenger, J. C., and O'Dowd, C.: Characterization of urban aerosol in Cork city (Ireland) using aerosol mass spectrometry, Atmos. Chem. Phys, 13, 4997-5015, 2013.

Falkovich, A. H., Graber, E. R., Schkolnik, G., Rudich, Y., Maenhaut, W., and Artaxo, P.: Low molecular weight organic acids in aerosol particles from Rondonia, Brazil, during the biomass-burning, transition and wet periods, Atmos. Chem. Phys, 5, 781-797, 2005.

Frank, N. H.: Retained nitrate, hydrated sulfates, and carbonaceous mass in Federal Reference Method fine particulate matter for six eastern cities, J. Air Waste Manage. Assoc., 56, 500-511, 2006.

Fujii, Y., Tohno, S., Amil, N., and Latif, M. T.: Quantitative assessment of source contributions to $PM_{2.5}$ on the west coast of Peninsular Malaysia to determine the burden of Indonesian peatland fire, Atmos. Environ., 171, 111-117, 2017.

Hennigan, C. J., Sullivan, A. P., Collett Jr., J. L., and Ronbinson, A. L.: Levoglucosan stability in biomass burning particles exposed to hydroxyl radicals, Geophysical Research Letters, 37, 1-4, 2010.

Hidy, G. M. and Friedlander, S. K.: The nature of the Los Angeles aerosol. In: Proceedings, Second International Clean Air Congress, Englund, H. M. and Beery, W. T. (Eds.), Academic Press, New York, 1971.

Hu, Y. Q., Fernandez-Anez, N., Smith, T. E. L., and Rein, G.: Review of emissions from smouldering peat fires and their contribution to regional haze episodes, International Journal of Wildland Fire, 27, 293-312, 2018.

Iinuma, Y., Bruggemann, E., Gnauk, T., Muller, K., Andreae, M. O., Helas, G., Parmar, R., and Herrmann, H.: Source characterization of biomass burning particles: The combustion of selected European conifers, African hardwood, savanna grass, and German and Indonesian peat, J. Geophys. Res. Atmos., 112, 2007.

Jayarathne, T., Stockwell, C. E., Gilbert, A. A., Daugherty, K., Cochrane, M. A., Ryan, K. C., Putra, E. I., Saharjo, B. H., Nurhayati, A. D., Albar, I., Yokelson, R. J., and Stone, E. A.: Chemical characterization of fine particulate matter emitted by peat fires in Central Kalimantan, Indonesia, during the 2015 El Nino, Atmos. Chem. Phys, 18, 2585-2600, 2018.

Jimenez, J. L.: Oxidation flow reactors (including PAM): Principles and best practices for applications in aerosol research, 2018 International Aerosol Conference Tutorial, St. Louis, MO, 2018. https://docs.google.com/viewer?a=v&pid=sites&srcid=ZGVmYXVsdGRvbWFpbnxwYW13aWtpfGd4OjY0N2MyYTZkYThiODU0MTM

Johnson, M. M.: Evaluatoin of a multiwavelength characterization of brown and black carbon from filter samples, M.S. Thesis, University of Nevada, Reno, Reno, NV, 2015.

Kang, E., Root, M. J., Toohey, D. W., and Brune, W. H.: Introducing the concept of Potential Aerosol Mass (PAM), Atmos. Chem. Phys, 7, 5727-5744, 2007.

Kessler, S. H., Smith, J. D., Che, D. L., Worsnop, D. R., Wilson, K. R., and Kroll, J. H.: Chemical sinks of organic aerosol: Kinetics and products of the heterogeneous oxidation of erythritol and levoglucosan, Environ. Sci. Technol., 44, 7005-7010, 2010.

Kourtchev, I., Hellebust, S., Bell, J. M., O'Connor, I. P., Healy, R. M., Allanic, A., Healy, D., Wenger, J. C., and Sodeau, J. R.: The use of polar organic compounds to estimate the contribution of domestic solid fuel combustion and biogenic sources to ambient levels of organic carbon and $PM_{2.5}$ in Cork Harbour, Ireland, Sci. Total Environ, 409, 2143-2155, 2011.

Kuo, L. J., Herbert, B. E., and Louchouarn, P.: Can levoglucosan be used to characterize and quantify char/charcoal black carbon in environmental media?, Organic Geochemistry, 39, 1466-1478, 2008.

Lai, C. Y., Liu, Y. C., Ma, J. Z., Ma, Q. X., and He, H.: Degradation kinetics of levoglucosan initiated by hydroxyl radical under different environmental conditions, Atmos. Environ., 91, 32-39, 2014.

Lambe, A. T., Ahern, A. T., Williams, L. R., Slowik, J. G., Wong, J. P. S., Abbatt, J. P. D., Brune, W. H., Ng, N. L., Wright, J. P., Croasdale, D. R., Worsnop, D. R., Davidovits, P., and Onasch, T. B.: Characterization of aerosol photooxidation flow reactors: heterogeneous oxidation, secondary organic aerosol formation and cloud condensation nuclei activity measurements, Atmos. Meas. Tech., 4, 445-461, 2011.

Li, R., Palm, B. B., Ortega, A. M., Hlywiak, J., Hu, W. W., Peng, Z., Day, D. A., Knote, C., Brune, W. H., de Gouw, J. A., and Jimenez, J. L.: Modeling the radical chemistry in an oxidation flow reactor: Radical formation and recycling, sensitivities, and the OH exposure estimation equation, Journal of Physical Chemistry A, 119, 4418-4432, 2015.

Lin, C. S., Ceburnis, D., Huang, R. J., Canonaco, F., Prevot, A. S. H., O'Dowd, C., and Ovadnevaite, J.: Summertime aerosol over the west of Ireland dominated by secondary aerosol during long-range transport, Atmosphere, 10, 2019.

Liu, Y. Y., Zhang, W. J., Bai, Z. P., Yang, W., Zhao, X. Y., Han, B., and Wang, X. H.: China Source Profile Shared Service (CSPSS): The Chinese $PM_{2.5}$ database for source profiles, Aerosol Air Qual. Res., 17, 1501-1514, 2017.

Louchouarn, P., Kuo, L. J., Wade, T. L., and Schantz, M.: Determination of levoglucosan and its isomers in size fractions of aerosol standard reference materials, Atmos. Environ., 43, 5630-5636, 2009.

Malm, W. C., Trijonis, J. C., Sisler, J. F., Pitchford, M. L., and Dennis, R. L.: Assessing the effect of SO_2 emission changes on visibility, Atmos. Environ., 28, 1023-1034, 1994.

Mao, J., Ren, X., Brune, W. H., Olson, J. R., Crawford, J. H., Fried, A., Huey, L. G., Cohen, R. C., Heikes, B., Singh, H. B., Blake, D. R., Sachse, G. W., Diskin, G. S., Hall, S. R., and Shetter, R. E.: Airborne measurement of OH reactivity during INTEX-B, Atmos. Chem. Phys, 9, 163-173, 2009.

May, A. A., Saleh, R., Hennigan, C. J., Donahue, N. M., and Robinson, A. L.: Volatility of organic molecular markers used for source apportionment analysis: Measurements and implications for atmospheric lifetime, Environ. Sci. Technol., 46, 12435-12444, 2012.

Mo, Z. W., Shao, M., and Lu, S. H.: Compilation of a source profile database for hydrocarbon and OVOC emissions in China, Atmos. Environ., 143, 209-217, 2016.

Nara, H., Tanimoto, H., Tohjima, Y., Mukai, H., Nojiri, Y., and Machida, T.: Emission factors of CO_2, CO and CH_4 from Sumatran peatland fires in 2013 based on shipboard measurements, Tellus Series B-Chemical and Physical Meteorology, 69, 2017.

PAMWiki: PAMWiki, 2019. https://sites.google.com/site/pamwiki/

Pant, P., Shukla, A., Kohl, S. D., Chow, J. C., Watson, J. G., and Harrison, R. M.: Characterization of ambient $PM_{2.5}$ at a pollution hotspot in New Delhi, India and inference of sources, Atmos. Environ., 109, 178-189, 2015.

Peng, Z., Day, D. A., Ortega, A. M., Palm, B. B., Hu, W. W., Stark, H., Li, R., Tsigaridis, K., Brune, W. H., and Jimenez, J. L.: Non-OH chemistry in oxidation flow reactors for the study of atmospheric chemistry systematically examined by modeling, Atmos. Chem. Phys, 16, 4283-4305, 2016.

Peng, Z., Day, D. A., Stark, H., Li, R., Lee-Taylor, J., Palm, B. B., Brune, W. H., and Jimenez, J. L.: HO_x radical chemistry in oxidation flow reactors with low-pressure mercury lamps systematically examined by modeling, Atmos. Meas. Tech., 8, 4863-4890, 2015.

Peng, Z. and Jimenez, J. L.: Modeling of the chemistry in oxidation flow reactors with high initial NO, Atmos. Chem. Phys., 17, 11991-12010, 2017.

Peng, Z., Palm, B. B., Day, D. A., Talukdar, R. K., Hu, W. W., Lambe, A. T., Brune, W. H., and Jimenez, J. L.: Model evaluation of new techniques for maintaining high-NO conditions in oxidation flow reactors for the study of OH-initiated atmospheric chemistry, Acs Earth and Space Chemistry, 2, 72-86, 2018.

Pernigotti, D., Belis, C. A., and Spanò, L.: SPECIEUROPE: The European data base for PM source profiles, Atmospheric Pollution Research, 7, 307-314, 2016.

Pratap, V., Bian, Q. J., Kiran, S. A., Hopke, P. K., Pierce, J. R., and Nakao, S.: Investigation of levoglucosan decay in wood smoke smog-chamber experiments: The importance of aerosol loading, temperature, and vapor wall losses in interpreting results, Atmos. Environ., 199, 224-232, 2019.

Reid, J. S., Eck, T. F., Christopher, S. A., Koppmann, R., Dubovik, O., Eleuterio, D. P., Holben, B. N., Reid, E. A., and Zhang, J.: A review of biomass burning emissions part III: intensive optical properties of biomass burning particles, Atmos. Chem. Phys, 5, 827-849, 2005.

Riggio, G. M., Chow, J. C., Cropper, P. M., Wang, X. L., Yatavelli, R. L. N., Yang, X. F., and Watson, J. G.: Feasibility of coupling a thermal/optical carbon analyzer to a quadrupole mass spectrometer for enhanced $PM_{2.5}$ speciation, J. Air Waste Manage. Assoc., 68, 463-476, 2018.

Rogula-Kozlowska, W., Klejnowski, K., Rogula-Kopiec, P., Mathews, B., and Szopa, S.: A study on the seasonal mass closure of ambient fine and coarse dusts in Zabrze, Poland, Bulletin of Environmental Contamination and Toxicology, 88, 722-729, 2012.

See, S. W., Balasubramanian, R., Rianawati, E., Karthikeyan, S., and Streets, D. G.: Characterization and source apportionment of particulate matter <= 2.5 mu m in Sumatra, Indonesia, during a recent peat fire episode, Environ. Sci. Technol., 41, 3488-3494, 2007.

Smith, J. D., Kroll, J. H., Cappa, C. D., Che, D. L., Liu, C. L., Ahmed, M., Leone, S. R., Worsnop, D. R., and Wilson, K. R.: The heterogeneous reaction of hydroxyl radicals with sub-micron squalane particles: a model system for understanding the oxidative aging of ambient aerosols, Atmos. Chem. Phys, 9, 3209-3222, 2009.

Stockwell, C. E., Jayarathne, T., Cochrane, M. A., Ryan, K. C., Putra, E. I., Saharjo, B. H., Nurhayati, A. D., Albar, I., Blake, D. R., Simpson, I. J., Stone, E. A., and Yokelson, R. J.: Field measurements of trace gases and aerosols emitted by peat fires in Central Kalimantan, Indonesia, during the 2015 El Nino, Atmos. Chem. Phys, 16, 11711-11732, 2016.

Stockwell, C. E., Yokelson, R. J., Kreidenweis, S. M., Robinson, A. L., Demott, P. J., Sullivan, R. C., Reardon, J., Ryan, K. C., Griffith, D. W. T., and Stevens, L.: Trace gas emissions from combustion of peat, crop residue, domestic biofuels, grasses, and other fuels: configuration and Fourier transform infrared (FTIR) component of the fourth Fire Lab at Missoula Experiment (FLAME-4), Atmos. Chem. Phys, 14, 9727-9754, 2014.

Stone, D., Whalley, L. K., and Heard, D. E.: Tropospheric OH and HO2 radicals: field measurements and model comparisons, Chemical Society Reviews, 41, 6348-6404, 2012.

Tham, J., Sarkar, S., Jia, S. G., Reid, J. S., Mishra, S., Sudiana, I. M., Swarup, S., Ong, C. N., and Yu, L. Y. E.: Impacts of peat-forest smoke on urban $PM_{2.5}$ in the Maritime Continent during 2012-2015: Carbonaceous profiles and indicators, Environ. Pollut., 248, 496-505, 2019.

Tian, J., Chow, J. C., Cao, J. J., Han, Y. M., Ni, H. Y., Chen, L.-W. A., Wang, X. L., Huang, R. J., Moosmüller, H., and Watson, J. G.: A biomass combustion chamber: Design, evaluation, and a case study of wheat straw combustion emission tests, Aerosol Air Qual. Res., 15, 2104-2114, 2015.

U.S.EPA: Guidance on the use of models and other analyses for demonstrating attainment of air quality goals for ozone, PM2.5, and regional haze, U.S. Environmental Protection Agency, Research Triangle Park, NC, 2007. http://www.epa.gov/ttn/scram/guidance/guide/final-03-pm-rh-guidance.pdf

U.S.EPA: SPECIATE Version 5.0, U.S. Environmental Protection Agency, Research Triangle Park, NC, 2019. https://www.epa.gov/air-emissions-modeling/speciate-version-45-through-40

Veres, P., Roberts, J. M., Burling, I. R., Warneke, C., de Gouw, J., and Yokelson, R. J.: Measurements of gas-phase inorganic and organic acids from biomass fires by negative-ion proton-transfer chemical-ionization mass spectrometry, J. Geophys. Res. Atmos., 115, 2010.

Watson, J. G.: Protocol for applying and validating the CMB model for $PM_{2.5}$ and VOC, U.S. Environmental Protection Agency, Research Triangle Park, NC, 2004. www.epa.gov/scram001/models/receptor/CMB_Protocol.pdf

Watson, J. G., Cao, J., Wang, Q., Tan, J., Li, L., Ho, S. S. H., Chen, L.-W. A., Watts, A. C., Wang, X. L., and Chow, J. C.: Gaseous, $PM_{2.5}$ mass, and speciated emission factors from laboratory chamber peat combustion, Atmospheric Chemistry and Physics Discussion, doi: 10.5194/acp-2019-456, 2019. online, 2019.

Watson, J. G., Chow, J. C., Engling, G., Chen, L.-W. A., and Wang, X. L.: Source apportionment: Principles and methods. In: Airborne Particulate Matter: Sources, Atmospheric Processes and Health, Harrison, R. M. (Ed.), Royal Society of Chemistry, London, UK, 2016.

Watson, J. G., Chow, J. C., and Frazier, C. A.: X-ray fluorescence analysis of ambient air samples. In: Elemental Analysis of Airborne Particles, Vol. 1, Landsberger, S. and Creatchman, M. (Eds.), Advances in Environmental, Industrial and Process Control Technologies, Gordon and Breach Science, Amsterdam, The Netherlands, 1999.

Watson, J. G., Chow, J. C., Wang, X. L., Kohl, S. D., Chen, L.-W. A., and Etyemezian, V. R.: Overview of real-world emission characterization methods. In: Alberta Oil Sands: Energy, Industry, and the Environment, Percy, K. E. (Ed.), Developments in Environmental Science, Elsevier Press, Amsterdam, The Netherlands, 2012.

Watson, J. G., Tropp, R. J., Kohl, S. D., Wang, X. L., and Chow, J. C.: Filter processing and gravimetric analysis for suspended particulate matter samples, Aerosol Science and Engineering, 1, 193-205, 2017.

Watson, J. G., Turpin, B. J., and Chow, J. C.: The measurement process: Precision, accuracy, and validity. In: Air Sampling Instruments for Evaluation of Atmospheric Contaminants, Ninth Edition, Cohen, B. S. and McCammon, C. S., Jr (Eds.), American Conference of Governmental Industrial Hygienists, Cincinnati, OH, 2001.

Wiggins, E. B., Czimczik, C. I., Santos, G. M., Chen, Y., Xu, X. M., Holden, S. R., Randerson, J. T., Harvey, C. F., Kai, F. M., and Yu, L. E.: Smoke radiocarbon measurements from Indonesian fires provide evidence for burning of millennia-aged peat, Proceedings of the National Academy of Sciences of the United States of America, 115, 12419-12424, 2018.

Table 1. Average fresh and aged peat combustion source profiles (in % of $PM_{2.5}$ mass) for six types of peats

	Average ± Standard Deviation of Percent $PM_{2.5}$ Mass[a]							
	Boreal							
	Odintsovo, Russia				Pskov, Siberia			
Aging Time	2 days		7 days		2 days		7 days	
	Fresh 2	Aged 2	Fresh 7	Aged 7	Fresh 2	Aged 2[b]	Fresh 7	Aged 7
Peat IDs in the average[c]	PEAT030, PEAT031, PEAT032		PEAT033, PEAT034, PEAT035		PEAT023, PEAT025, PEAT026		PEAT027, PEAT028, PEAT029	
Nitric Acid (HNO_3)	0.18 ± 0.080	0.32 ± 0.15	0.21 ± 0.059	0.24 ± 0.085	0.18 ± 0.052	0.27 ± 0.074	0.27 ± 0.075	0.39 ± 0.15
Ammonia (NH_3)	6.0095 ± 0.93	3.21 ± 0.78	7.84 ± 0.31	4.56 ± 1.36	18.21 ± 3.97	8.81 ± 4.047	22.81 ± 5.88	7.090 ± 5.59
Water-Soluble Sodium (Na^+)	0.018 ± 0.0015	0.024 ± 0.0013	0.022 ± 0.011	0.032 ± 0.0074	0.017 ± 0.0011	0.047 ± 0.020	0.0688 ± 0.038	0.058 ± 0.053
Water-Soluble Potassium (K^+)	0.034 ± 0.036	na[d]	0.11 ± 0.087	na[d]	0.020 ± 0.016	na[d]	0.0230 ± 0.014	na[d]
Chloride (Cl^-)	0.16 ± 0.022	0.12 ± 0.019	0.25 ± 0.053	0.092 ± 0.011	0.11 ± 0.031	0.11 ± 0.048	0.17 ± 0.014	0.086 ± 0.033
Nitrite (NO_2^-)	0.037 ± 0.063	0.00095 ± 0.0016	0.00 ± 0.00028	0.00086 ± 0.00077	0.0013 ± 0.0023	0.0023 ± 0.0036	0.20 ± 0.34	0.0056 ± 0.0033
Nitrate (NO_3^-)	0.23 ± 0.20	0.74 ± 0.080	0.13 ± 0.043	2.0029 ± 0.71	0.11 ± 0.11	1.79 ± 0.52	0.15 ± 0.076	8.23 ± 4.34
Sulfate ($SO_4^{=}$)	0.30 ± 0.33	0.67 ± 0.46	0.15 ± 0.044	0.84 ± 0.24	0.28 ± 0.15	0.68 ± 0.19	0.27 ± 0.025	1.15 ± 0.63
Ammonium (NH_4^+)	0.13 ± 0.14	1.045 ± 0.93	0.097 ± 0.057	3.38 ± 1.38	0.0014 ± 0.0012	0.21 ± 0.18	0.0463 ± 0.044	6.66 ± 3.67
OC1 (140°C)	11.82 ± 2.58	6.42 ± 3.94	15.67 ± 3.60	4.096 ± 0.72	11.81 ± 2.20	5.014 ± 0.70	11.40 ± 0.65	4.34 ± 1.69
OC2 (280°C)	13.16 ± 1.42	9.84 ± 1.094	12.029 ± 1.049	9.032 ± 1.27	20.59 ± 1.87	15.45 ± 2.65	21.21 ± 2.38	10.54 ± 0.18
OC3 (480°C)	17.69 ± 3.013	14.60 ± 1.93	17.33 ± 2.39	13.99 ± 2.46	25.93 ± 3.62	26.78 ± 8.46	29.63 ± 5.62	19.74 ± 0.79
OC4 (580°C)	6.69 ± 0.49	5.83 ± 0.51	6.090 ± 1.61	4.40 ± 0.84	5.79 ± 0.21	8.85 ± 1.27	8.72 ± 3.83	6.31 ± 2.35
Pyrolized Carbon (OP)	8.26 ± 2.086	8.61 ± 4.35	9.29 ± 1.0016	9.39 ± 1.30	9.52 ± 2.15	12.12 ± 4.27	10.34 ± 1.82	12.76 ± 1.58
Organic Carbon (OC)[g]	57.61 ± 5.21	45.29 ± 9.90	60.42 ± 5.37	40.90 ± 4.87	73.65 ± 6.82	68.21 ± 13.33	81.30 ± 9.29	53.69 ± 5.32
EC1 (580°C)	6.47 ± 1.64	6.77 ± 2.33	6.51 ± 0.53	9.31 ± 1.50	7.84 ± 2.19	9.23 ± 0.82	5.31 ± 0.57	7.79 ± 1.28
EC2 (740°C)	3.60 ± 2.32	3.36 ± 2.52	4.61 ± 0.034	2.051 ± 0.50	4.92 ± 3.76	5.98 ± 4.73	5.87 ± 0.74	7.038 ± 2.48
EC3 (840°C)	0.00 ± 0.00020	0.00 ± 0.00022	0.00 ± 0.00020	0.00 ± 0.00021	0.00 ± 0.00021	0.00 ± 0.00028	0.00 ± 0.00029	0.00 ± 0.00032
Elemental Carbon (EC)[g]	1.82 ± 1.26	1.52 ± 0.36	1.83 ± 0.69	1.98 ± 0.75	3.23 ± 0.80	3.090 ± 0.83	0.83 ± 1.30	2.076 ± 0.36
Total Carbon (TC)	59.43 ± 4.49	46.81 ± 10.23	62.25 ± 4.95	42.88 ± 4.76	76.88 ± 6.37	71.30 ± 13.96	82.14 ± 10.57	55.77 ± 5.58
Water-Soluble OC (WSOC)	36.97 ± 2.71	31.80 ± 3.15	35.77 ± 2.30	29.21 ± 6.31	23.84 ± 1.84	29.88 ± 7.10	32.50 ± 0.71[e]	29.88 ± 8.88
Formic acid (CH_2O_2)	0.17 ± 0.074	0.23 ± 0.054	0.23 ± 0.090	0.32 ± 0.18	0.045 ± 0.016	0.18 ± 0.054	0.067 ± 0.0097	0.44 ± 0.28
Acetic acid ($C_2H_4O_2$)	0.61 ± 0.38	0.63 ± 0.37	0.67 ± 0.15	0.88 ± 0.47	0.20 ± 0.16	0.34 ± 0.15	0.23 ± 0.15	1.46 ± 2.03
Oxalic acid ($C_2H_2O_4$)	0.10 ± 0.063	0.97 ± 0.20	0.28 ± 0.22	2.88 ± 0.77	0.062 ± 0.013	1.31 ± 0.47	0.076 ± 0.019	3.90 ± 1.43
Propionic acid ($C_3H_5O_2$)	0.036 ± 0.032	0.12 ± 0.15	0.066 ± 0.032	0.020 ± 0.031	0.00 ± 0.00015	0.026 ± 0.045	0.032 ± 0.032	0.00 ± 0.00023
Levoglucosan ($C_6H_{10}O_5$)	35.35 ± 7.90	24.95 ± 8.97	38.66 ± 2.089	19.63 ± 4.044	6.66 ± 2.58	4.21 ± 0.59	9.39 ± 2.077	3.80 ± 0.35
Mannosan ($C_6H_{10}O_5$)	3.93 ± 1.18	2.52 ± 1.068	5.039 ± 0.58	2.14 ± 0.85	0.053 ± 0.092	0.00 ± 0.00044	1.28 ± 0.54	0.46 ± 0.16
Galactose/Maltitol ($C_6H_{12}O_6$/$C_{12}H_{24}O_{11}$)	0.00 ± 0.00016	0.00 ± 0.00017	0.063 ± 0.11	0.00 ± 0.00016	0.0058 ± 0.010	0.00 ± 0.00023	0.00 ± 0.00023	0.082 ± 0.14
Glycerol ($C_3H_8O_3$)	1.90 ± 0.19	1.73 ± 0.42	3.54 ± 2.14	1.25 ± 0.17	0.00 ± 0.0000029	0.00 ± 0.0000040	0.43 ± 0.43	0.00 ± 0.0000046
Mannitol ($C_6H_{14}O_6$)	0.00 ± 0.000056	0.00 ± 0.000061	0.062 ± 0.11	0.00 ± 0.000058	0.00 ± 0.000058	0.00 ± 0.000081	0.00 ± 0.0000836	0.17 ± 0.30
Aluminum (Al)	0.073 ± 0.66	0.15 ± 0.87	0.22 ± 0.73	0.29 ± 2.74	0.086 ± 1.49	0.00 ± 0.0074	0.075 ± 0.83	0.20 ± 0.17
Silicon (Si)	0.0069 ± 0.12	0.12 ± 0.44	0.013 ± 0.12	0.68 ± 0.24	0.022 ± 0.19	0.22 ± 0.00089	0.0050 ± 0.044	0.47 ± 0.79
Phosphorous (P)	0.00 ± 0.000084	0.00018 ± 0.00025	0.00079 ± 0.0014	0.00 ± 0.000095	0.00 ± 0.000090	0.00 ± 0.00017	0.00 ± 0.00012	0.00 ± 0.000093

Table 1 (cont'd)

	Average ± Standard Deviation of Percent $PM_{2.5}$ Mass[a]							
	Boreal							
	Odintsovo, Russia				Pskov, Siberia			
Aging Time	2 days		7 days		2 days		7 days	
	Fresh 2	Aged 2	Fresh 7	Aged 7	Fresh 2	Aged 2[b]	Fresh 7	Aged 7
Peat IDs in the average[c]	PEAT030, PEAT031, PEAT032		PEAT033, PEAT034, PEAT035		PEAT023, PEAT025, PEAT026		PEAT027, PEAT028, PEAT029	
Sulfur (S)	0.024 ± 0.0088	0.081 ± 0.046	0.040 ± 0.056	0.26 ± 0.095	0.081 ± 0.030	0.090 ± 0.000098	0.028 ± 0.034	0.31 ± 0.0057
Chlorine (Cl)	0.12 ± 0.027	0.035 ± 0.019	0.18 ± 0.030	0.032 ± 0.0025	0.11 ± 0.015	0.057 ± 0.000068	0.081 ± 0.018	0.027 ± 0.0064
Potassium (K)	0.030 ± 0.011	0.48 ± 0.44	0.041 ± 0.018	0.13 ± 0.035	0.15 ± 0.19	0.096 ± 0.00025	0.11 ± 0.14	0.30 ± 0.017
Calcium (Ca)	0.018 ± 0.016	0.040 ± 0.056	0.031 ± 0.025	0.0034 ± 0.0048	0.00 ± 0.00	0.00 ± 0.00092	0.00 ± 0.00065	0.028 ± 0.039
Scandium (Sc)	0.064 ± 0.11	0.00 ± 0.0021	0.00 ± 0.0021	0.00 ± 0.0023	0.079 ± 0.14	0.00 ± 0.0041	0.031 ± 0.053	0.00 ± 0.0022
Titanium (Ti)	0.0046 ± 0.0056	0.00 ± 0.000076	0.0055 ± 0.0049	0.0013 ± 0.0018	0.0079 ± 0.014	0.00 ± 0.00015	0.00 ± 0.00010	0.00 ± 0.000078
Vanadium (V)	0.00 ± 0.000013	0.00 ± 0.000014	0.00 ± 0.000014	0.00 ± 0.000015	0.00070 ± 0.0012	0.00 ± 0.000027	0.00 ± 0.000019	0.00 ± 0.000015
Chromium (Cr)	0.0012 ± 0.0020	0.00039 ± 0.00056	0.00 ± 0.000046	0.00084 ± 0.0012	0.00079 ± 0.0014	0.00 ± 0.000091	0.0010 ± 0.00095	0.00 ± 0.000049
Manganese (Mn)	0.0014 ± 0.0022	0.00053 ± 0.00074	0.0037 ± 0.0033	0.00 ± 0.00018	0.0018 ± 0.0022	0.020 ± 0.00032	0.0031 ± 0.0031	0.0051 ± 0.0072
Iron (Fe)	0.038 ± 0.021	0.091 ± 0.098	0.062 ± 0.043	0.26 ± 0.32	0.039 ± 0.035	0.029 ± 0.00056	0.013 ± 0.017	0.015 ± 0.021
Cobalt (Co)	0.000032 ± 0.000056	0.00 ± 0.0000094	0.000037 ± 0.000064	0.00049 ± 0.00069	0.00018 ± 0.00031	0.00 ± 0.000018	0.00 ± 0.000013	0.00 ± 0.000018
Nickel (Ni)	0.00 ± 0.000022	0.0026 ± 0.0037	0.000029 ± 0.000050	0.00 ± 0.000025	0.00 ± 0.000024	0.00086 ± 0.000045	0.0014 ± 0.0017	0.00041 ± 0.00039
Copper (Cu)	0.0055 ± 0.0029	0.15 ± 0.11	0.0052 ± 0.0038	0.046 ± 0.054	0.0072 ± 0.0041	0.014 ± 0.00028	0.047 ± 0.052	0.11 ± 0.067
Zinc (Zn)	0.0017 ± 0.0015	0.054 ± 0.066	0.0047 ± 0.0041	0.053 ± 0.070	0.0053 ± 0.0030	0.0034 ± 0.00016	0.0058 ± 0.0056	0.0019 ± 0.00081
Arsenic (As)	0.00086 ± 0.0015	0.00 ± 0.000038	0.00 ± 0.000037	0.00 ± 0.000040	0.00076 ± 0.0013	0.0050 ± 0.000073	0.000069 ± 0.00012	0.00013 ± 0.00019
Selenium (Se)	0.00021 ± 0.00036	0.0026 ± 0.0037	0.00067 ± 0.00076	0.00029 ± 0.00041	0.0018 ± 0.0022	0.0026 ± 0.00013	0.00035 ± 0.00031	0.00029 ± 0.00041
Bromine (Br)	0.00041 ± 0.00036	0.0030 ± 0.0031	0.00096 ± 0.0014	0.0021 ± 0.0019	0.0072 ± 0.0043	0.0032 ± 0.000036	0.0092 ± 0.0066	0.0066 ± 0.0014
Rubidium (Rb)	0.00052 ± 0.00090	0.0029 ± 0.000079	0.0020 ± 0.0019	0.00049 ± 0.00069	0.00031 ± 0.00054	0.00 ± 0.000045	0.00066 ± 0.00068	0.0024 ± 0.0034
Strontium (Sr)	0.0033 ± 0.0032	0.0017 ± 0.0018	0.0032 ± 0.0027	0.0033 ± 0.0013	0.0027 ± 0.0028	0.0039 ± 0.000045	0.0072 ± 0.0042	0.0047 ± 0.0066
Yttrium (Y)	0.00079 ± 0.0013	0.000066 ± 0.000093	0.0031 ± 0.0035	0.00077 ± 0.0011	0.0014 ± 0.0012	0.0015 ± 0.000045	0.0045 ± 0.0045	0.0053 ± 0.0049
Zirconium (Zr)	0.0040 ± 0.0024	0.0034 ± 0.0014	0.0013 ± 0.0018	0.0017 ± 0.0024	0.0051 ± 0.0019	0.00 ± 0.00017	0.0060 ± 0.0088	0.0033 ± 0.0021
Niobium (Nb)	0.00072 ± 0.0012	0.0023 ± 0.0013	0.00036 ± 0.00038	0.00063 ± 0.00089	0.00040 ± 0.00069	0.00064 ± 0.000082	0.00039 ± 0.00067	0.00044 ± 0.00062
Molybdenum (Mo)	0.0020 ± 0.0035	0.00 ± 0.000090	0.0015 ± 0.0011	0.0030 ± 0.0010	0.0029 ± 0.0051	0.00 ± 0.00017	0.0013 ± 0.0022	0.0026 ± 0.0037
Silver (Ag)	0.0010 ± 0.0015	0.00 ± 0.00011	0.00 ± 0.00011	0.00 ± 0.00012	0.00 ± 0.00011	0.00 ± 0.00022	0.0083 ± 0.0074	0.00 ± 0.00012
Cadmium (Cd)	0.0034 ± 0.0059	0.0038 ± 0.0053	0.0023 ± 0.0039	0.0023 ± 0.0033	0.00 ± 0.00016	0.00 ± 0.00030	0.0024 ± 0.0029	0.00 ± 0.00016
Indium (In)	0.00 ± 0.00010	0.00 ± 0.00011	0.0059 ± 0.0011	0.0060 ± 0.0016	0.00065 ± 0.0011	0.018 ± 0.00021	0.0027 ± 0.0047	0.00 ± 0.00011
Tin (Sn)	0.0028 ± 0.0048	0.0095 ± 0.013	0.0013 ± 0.0022	0.0037 ± 0.0053	0.0098 ± 0.010	0.0075 ± 0.00038	0.0092 ± 0.014	0.0089 ± 0.013
Antimony (Sb)	0.00 ± 0.00028	0.0086 ± 0.012	0.00 ± 0.00029	0.00 ± 0.00032	0.00 ± 0.00030	0.000053 ± 0.00058	0.00 ± 0.00041	0.00 ± 0.00031
Cesium (Cs)	0.025 ± 0.040	0.0085 ± 0.012	0.023 ± 0.033	0.014 ± 0.020	0.0057 ± 0.0099	0.00 ± 0.0016	0.0046 ± 0.0079	0.00 ± 0.00086
Barium (Ba)	0.014 ± 0.024	0.00 ± 0.00071	0.011 ± 0.020	0.00 ± 0.00068	0.023 ± 0.020	0.00 ± 0.0012	0.00 ± 0.00086	0.00 ± 0.0067
Lanthanum (La)	0.048 ± 0.043	0.00 ± 0.0012	0.049 ± 0.043	0.059 ± 0.083	0.017 ± 0.030	0.00 ± 0.0024	0.094 ± 0.085	0.020 ± 0.028
Wolfram (W)	0.0023 ± 0.0014	0.0073 ± 0.010	0.0077 ± 0.013	0.011 ± 0.0016	0.00079 ± 0.0014	0.00 ± 0.00047	0.0047 ± 0.0082	0.0048 ± 0.00054
Gold (Au)	0.0029 ± 0.0027	0.00 ± 0.000071	0.00080 ± 0.0014	0.0024 ± 0.0033	0.00 ± 0.000071	0.012 ± 0.00014	0.0038 ± 0.0065	0.0018 ± 0.0025
Mercury (Hg)	0.0015 ± 0.0014	0.00 ± 0.000038	0.00081 ± 0.0014	0.00 ± 0.000040	0.0013 ± 0.0023	0.00 ± 0.000073	0.000065 ± 0.00011	0.00 ± 0.000039
Lead (Pb)	0.0026 ± 0.0024	0.0018 ± 0.0025	0.0024 ± 0.0028	0.0053 ± 0.0074	0.00 ± 0.000071	0.00 ± 0.00014	0.0050 ± 0.00088	0.0027 ± 0.0032
Uranium (U)	0.0018 ± 0.0031	0.0017 ± 0.0024	0.00096 ± 0.0017	0.0024 ± 0.0035	0.0028 ± 0.0027	0.00 ± 0.00025	0.0025 ± 0.0033	0.0046 ± 0.0066

Table 1 (cont'd)

	Average ± Standard Deviation of Percent $PM_{2.5}$ Mass							
	Temperate				Subtropical			
	Northern Alaska, USA				Putnam County Lakebed, Florida (FL1)			
Aging Time	2 days		7 days		2 (25%) days		7 (25%) days	
	Fresh 2	Aged 2	Fresh 7	Aged 7[b]	Fresh 2	Aged 2	Fresh 7	Aged 7
Peat IDs in the average[c]	PEAT013, PEAT014, PEAT019		PEAT020, PEAT022		PEAT008, PEAT009		PEAT005, PEAT006	
Nitric Acid (HNO_3)	0.40 ± 0.19	0.31 ± 0.15	0.29 ± 0.22	0.28 ± 0.10	0.18 ± 0.033	0.39 ± 0.17	0.32 ± 0.25	0.23 ± 0.0055
Ammonia (NH_3)	16.64 ± 8.41	6.39 ± 3.76	27.73 ± 11.16	5.13 ± 0.80	28.03 ± 2.90	4.76 ± 0.52	na[f]	1.39 ± 0.62
Water-Soluble Sodium (Na^+)	0.047 ± 0.035	0.13 ± 0.15	0.047 ± 0.036	0.053 ± 0.022	0.015 ± 0.00033	0.033 ± 0.00033	0.030 ± 0.0058	0.032 ± 0.0048
Water-Soluble Potassium (K^+)	0.042 ± 0.068	na[d]	0.035 ± 0.010	na[d]	0.010 ± 0.015	na[d]	0.029 ± 0.0042	na[d]
Chloride (Cl^-)	0.21 ± 0.050	0.25 ± 0.19	0.29 ± 0.029	0.11 ± 0.0042	0.14 ± 0.035	0.18 ± 0.10	0.14 ± 0.041	0.087 ± 0.0049
Nitrite (NO_2^-)	0.15 ± 0.25	0.0015 ± 0.0019	0.00 ± 0.00040	0.0014 ± 0.00094	0.053 ± 0.071	0.011 ± 0.015	0.00044 ± 0.00062	0.0012 ± 0.00037
Nitrate (NO_3^-)	0.20 ± 0.16	1.45 ± 0.79	0.17 ± 0.053	8.19 ± 5.96	0.16 ± 0.12	0.87 ± 0.15	0.040 ± 0.000070	1.10 ± 0.18
Sulfate ($SO_4^{=}$)	0.46 ± 0.38	0.35 ± 0.16	0.26 ± 0.24	0.64 ± 0.23	0.89 ± 0.97	1.60 ± 1.33	0.22 ± 0.013	1.29 ± 0.13
Ammonium (NH_4^+)	0.11 ± 0.19	0.66 ± 0.78	0.0028 ± 0.00085	4.30 ± 0.098	0.00070 ± 0.00099	0.052 ± 0.074	0.00046 ± 0.000031	1.0080 ± 0.048
OC1 (140°C)	14.58 ± 4.92	10.33 ± 4.49	9.28 ± 4.049	3.76 ± 1.77	9.54 ± 2.50	7.48 ± 3.12	13.15 ± 3.56	10.087 ± 1.63
OC2 (280°C)	21.37 ± 0.70	17.98 ± 1.13	17.28 ± 3.42	9.68 ± 3.57	21.66 ± 2.045	19.50 ± 0.85	20.74 ± 2.34	19.76 ± 2.57
OC3 (480°C)	26.36 ± 5.88	24.57 ± 6.14	28.99 ± 14.35	18.47 ± 5.013	25.30 ± 7.61	24.97 ± 0.95	20.38 ± 0.63	21.97 ± 1.65
OC4 (580°C)	7.70 ± 1.79	6.51 ± 1.99	8.0014 ± 4.44	8.56 ± 2.51	7.60 ± 4.045	7.76 ± 1.017	4.29 ± 0.0044	5.34 ± 2.10
Pyrolized Carbon (OP)	7.40 ± 1.69	10.66 ± 4.45	7.35 ± 2.14	6.68 ± 3.39	7.61 ± 1.80	10.45 ± 1.14	8.81 ± 0.79	10.73 ± 0.53
Organic Carbon (OC)[g]	77.41 ± 6.13	70.047 ± 8.98	70.91 ± 20.30	47.16 ± 11.23	71.71 ± 9.40	70.16 ± 5.033	67.37 ± 4.48	67.88 ± 5.22
EC1 (580°C)	6.050 ± 1.50	9.94 ± 2.92	5.24 ± 1.038	7.11 ± 3.90	7.61 ± 2.43	9.58 ± 1.36	6.44 ± 0.099	8.98 ± 1.36
EC2 (740°C)	3.43 ± 3.013	2.93 ± 2.14	5.70 ± 1.85	1.63 ± 1.99	3.51 ± 2.51	2.94 ± 2.34	4.057 ± 0.60	3.28 ± 0.88
EC3 (840°C)	0.00 ± 0.00020	0.00 ± 0.00021	0.00 ± 0.00029	0.00 ± 0.00022	0.00 ± 0.00014	0.00 ± 0.00015	0.00 ± 0.00011	0.00 ± 0.00010
Elemental Carbon (EC)[g]	2.082 ± 1.079	2.21 ± 0.99	3.59 ± 0.75	2.047 ± 2.51	3.51 ± 1.72	2.076 ± 0.16	1.69 ± 0.29	1.53 ± 0.057
Total Carbon (TC)	79.49 ± 7.072	72.26 ± 8.88	74.50 ± 21.052	49.20 ± 13.74	75.23 ± 11.12	72.24 ± 4.88	69.06 ± 4.77	69.41 ± 5.16
Water-Soluble OC (WSOC)	29.32 ± 9.03	28.35 ± 3.81	31.58 ± 11.22	25.77 ± 4.05	19.53 ± 4.67	22.71 ± 4.43	16.33 ± 1.17	23.15 ± 1.45
Formic acid (CH_2O_2)	0.093 ± 0.029	0.21 ± 0.049	0.069 ± 0.018	0.25 ± 0.11	0.11 ± 0.097	0.20 ± 0.13	0.022 ± 0.0044	0.15 ± 0.0065
Acetic acid ($C_2H_4O_2$)	0.38 ± 0.15	0.64 ± 0.17	0.45 ± 0.24	0.34 ± 0.26	0.19 ± 0.15	0.047 ± 0.011	0.056 ± 0.010	0.26 ± 0.024
Oxalic acid ($C_2H_2O_4$)	0.039 ± 0.028	0.86 ± 0.16	0.043 ± 0.061	3.26 ± 0.52	0.050 ± 0.070	0.58 ± 0.26	0.00 ± 0.02	1.12 ± 0.19
Propionic acid ($C_3H_5O_2$)	0.0072 ± 0.010	0.024 ± 0.034	0.00 ± 0.00020	0.034 ± 0.048	0.00 ± 0.000099	0.00 ± 0.00010	0.00 ± 0.000077	0.00 ± 0.000071
Levoglucosan ($C_6H_{10}O_5$)	17.87 ± 8.03	16.99 ± 3.32	9.78 ± 1.15	4.87 ± 2.89	3.15 ± 0.0092	2.78 ± 0.041	3.12 ± 0.24	1.49 ± 0.50
Mannosan ($C_6H_{10}O_5$)	3.46 ± 1.25	3.53 ± 1.26	2.73 ± 0.40	0.95 ± 0.34	0.00 ± 0.00022	0.00 ± 0.00023	0.00 ± 0.00017	0.00 ± 0.00016
Galactose/Maltitol ($C_6H_{12}O_6$/$C_{12}H_{24}O_{11}$)	0.00 ± 0.00015	0.00 ± 0.00016	0.00 ± 0.00022	0.00 ± 0.00017	0.00 ± 0.00011	0.00 ± 0.00012	0.00 ± 0.00087	0.00 ± 0.000079
Glycerol ($C_3H_8O_3$)	0.23 ± 0.33	0.20 ± 0.28	0.98 ± 1.39	0.12 ± 0.17	0.00 ± 0.0000050	0.00 ± 0.0000021	0.00 ± 0.0000015	0.00 ± 0.0000014
Mannitol ($C_6H_{14}O_6$)	0.00 ± 0.000055	0.10 ± 0.15	0.00 ± 0.000080	0.00 ± 0.000061	0.00 ± 0.000039	0.00 ± 0.000042	0.00 ± 0.000056	0.00 ± 0.000028
Aluminum (Al)	0.026 ± 0.24	0.063 ± 0.28	0.029 ± 0.13	0.0098 ± 0.0046	0.026 ± 0.059	0.069 ± 0.97	0.12 ± 1.34	0.080 ± 0.61
Silicon (Si)	0.0077 ± 0.12	0.0069 ± 0.098	0.0012 ± 0.017	0.63 ± 0.00060	0.00 ± 0.00030	0.021 ± 0.22	0.00 ± 0.0021	0.021 ± 0.067
Phosphorous (P)	0.00 ± 0.000084	0.00 ± 0.00011	0.00 ± 0.00012	0.00 ± 0.00011	0.00 ± 0.000060	0.00 ± 0.000064	0.00 ± 0.000048	0.00 ± 0.000044

Table 1 (cont'd)

	Average ± Standard Deviation of Percent $PM_{2.5}$ Mass							
	Temperate				Subtropical			
	Northern Alaska, USA				Putnam County Lakebed, Florida (FL1)			
Aging Time	2 days		7 days		2 (25%) days		7 (25%) days	
	Fresh 2	Aged 2	Fresh 7	Aged 7[b]	Fresh 2	Aged 2	Fresh 7	Aged 7
Peat IDs in the average[c]	PEAT013, PEAT014, PEAT019		PEAT020, PEAT022		PEAT008, PEAT009		PEAT005, PEAT006	
Sulfur (S)	0.031 ± 0.054	0.062 ± 0.087	0.0099 ± 0.014	0.34 ± 0.00013	0.19 ± 0.056	0.37 ± 0.24	0.17 ± 0.037	0.74 ± 0.047
Chlorine (Cl)	0.12 ± 0.068	0.087 ± 0.030	0.14 ± 0.049	0.019 ± 0.000040	0.12 ± 0.0064	0.067 ± 0.024	0.14 ± 0.022	0.056 ± 0.00047
Potassium (K)	0.046 ± 0.016	0.16 ± 0.15	0.052 ± 0.046	0.47 ± 0.00022	0.0092 ± 0.012	0.057 ± 0.035	0.0046 ± 0.00044	0.12 ± 0.10
Calcium (Ca)	0.032 ± 0.032	0.032 ± 0.045	0.035 ± 0.049	0.00 ± 0.00057	0.0040 ± 0.0056	0.00 ± 0.00034	0.00 ± 0.00025	0.00 ± 0.00023
Scandium (Sc)	0.00 ± 0.0020	0.00 ± 0.0025	0.00 ± 0.0029	0.00 ± 0.0026	0.00 ± 0.0014	0.00 ± 0.0015	0.022 ± 0.031	0.00 ± 0.0010
Titanium (Ti)	0.00 ± 0.000071	0.00 ± 0.000091	0.0055 ± 0.0078	0.051 ± 0.000093	0.0036 ± 0.0050	0.00 ± 0.000054	0.0086 ± 0.012	0.00 ± 0.000037
Vanadium (V)	0.00 ± 0.000013	0.00 ± 0.000017	0.00 ± 0.000019	0.00 ± 0.000017	0.00 ± 0.000094	0.00 ± 0.000010	0.00 ± 0.0000075	0.00 ± 0.0000069
Chromium (Cr)	0.00051 ± 0.00089	0.00028 ± 0.00040	0.00 ± 0.000065	0.00 ± 0.000057	0.00 ± 0.000032	0.00 ± 0.000034	0.00034 ± 0.00048	0.00 ± 0.000023
Manganese (Mn)	0.0015 ± 0.0014	0.00069 ± 0.00098	0.0016 ± 0.0023	0.0011 ± 0.00020	0.0013 ± 0.0012	0.00033 ± 0.00047	0.00057 ± 0.00080	0.0016 ± 0.0018
Iron (Fe)	0.036 ± 0.014	0.10 ± 0.095	0.049 ± 0.048	0.029 ± 0.00035	0.00 ± 0.00019	0.047 ± 0.040	0.024 ± 0.012	0.065 ± 0.0091
Cobalt (Co)	0.00 ± 0.0000088	0.00 ± 0.000011	0.00 ± 0.000013	0.00013 ± 0.000011	0.00 ± 0.0000063	0.00021 ± 0.00030	0.00020 ± 0.00028	0.00 ± 0.0000046
Nickel (Ni)	0.00028 ± 0.00049	0.00 ± 0.000028	0.00075 ± 0.0011	0.00 ± 0.000028	0.00045 ± 0.00064	0.00 ± 0.000017	0.00069 ± 0.00097	0.00043 ± 0.00026
Copper (Cu)	0.028 ± 0.047	0.027 ± 0.034	0.0098 ± 0.0028	0.15 ± 0.00018	0.00 ± 0.000098	0.0035 ± 0.0049	0.0019 ± 0.0000053	0.069 ± 0.090
Zinc (Zn)	0.026 ± 0.036	0.027 ± 0.031	0.0026 ± 0.0020	0.011 ± 0.000097	0.0013 ± 0.0015	0.0023 ± 0.0032	0.00041 ± 0.000028	0.0046 ± 0.00037
Arsenic (As)	0.0006 ± 0.00078	0.00 ± 0.000045	0.00 ± 0.000052	0.00067 ± 0.000045	0.00 ± 0.000025	0.00 ± 0.000027	0.000062 ± 0.000087	0.00034 ± 0.00048
Selenium (Se)	0.00016 ± 0.00028	0.0064 ± 0.0017	0.0022 ± 0.0032	0.00 ± 0.000080	0.0017 ± 0.00092	0.00 ± 0.000047	0.00034 ± 0.00048	0.0034 ± 0.0017
Bromine (Br)	0.0017 ± 0.0018	0.0031 ± 0.0044	0.0079 ± 0.00064	0.0020 ± 0.000023	0.020 ± 0.00098	0.0077 ± 0.010	0.024 ± 0.0043	0.019 ± 0.0012
Rubidium (Rb)	0.00 ± 0.000022	0.0035 ± 0.0048	0.0057 ± 0.0059	0.0026 ± 0.000028	0.00011 ± 0.00016	0.00095 ± 0.0013	0.00 ± 0.000013	0.00066 ± 0.00047
Strontium (Sr)	0.0017 ± 0.00036	0.0076 ± 0.0084	0.0068 ± 0.0014	0.0028 ± 0.000028	0.0023 ± 0.00057	0.0038 ± 0.0013	0.0018 ± 0.00075	0.0046 ± 0.0025
Yttrium (Y)	0.0013 ± 0.0014	0.0037 ± 0.0013	0.0057 ± 0.0041	0.0054 ± 0.000028	0.0014 ± 0.00029	0.0012 ± 0.0018	0.00085 ± 0.000067	0.0022 ± 0.0032
Zirconium (Zr)	0.0027 ± 0.0028	0.0047 ± 0.0014	0.0025 ± 0.0027	0.011 ± 0.00011	0.0016 ± 0.0023	0.0003 ± 0.00089	0.00074 ± 0.0010	0.0013 ± 0.00079
Niobium (Nb)	0.00 ± 0.000040	0.00092 ± 0.00090	0.00027 ± 0.00039	0.00 ± 0.000051	0.0016 ± 0.0023	0.00082 ± 0.0012	0.00042 ± 0.00060	0.00 ± 0.000021
Molybdenum (Mo)	0.0012 ± 0.0019	0.0044 ± 0.0062	0.0020 ± 0.00084	0.00 ± 0.00011	0.00 ± 0.000060	0.00063 ± 0.00089	0.0025 ± 0.00092	0.00 ± 0.000044
Silver (Ag)	0.00 ± 0.00011	0.00 ± 0.00014	0.00 ± 0.00016	0.00 ± 0.00014	0.0010 ± 0.0014	0.00 ± 0.000081	0.00 ± 0.000060	0.00 ± 0.000055
Cadmium (Cd)	0.00 ± 0.00015	0.00 ± 0.00019	0.00 ± 0.00022	0.00 ± 0.00019	0.0034 ± 0.0049	0.00 ± 0.00011	0.0029 ± 0.00093	0.0020 ± 0.0029
Indium (In)	0.00082 ± 0.0013	0.0011 ± 0.0016	0.00069 ± 0.00097	0.00 ± 0.00013	0.00068 ± 0.00096	0.0025 ± 0.0036	0.0021 ± 0.0030	0.0018 ± 0.0026
Tin (Sn)	0.0045 ± 0.0078	0.014 ± 0.020	0.0067 ± 0.0025	0.00 ± 0.00024	0.0037 ± 0.00047	0.0034 ± 0.0048	0.0028 ± 0.0025	0.0074 ± 0.00049
Antimony (Sb)	0.0065 ± 0.011	0.015 ± 0.021	0.00 ± 0.00041	0.00 ± 0.00036	0.00 ± 0.00020	0.0072 ± 0.010	0.0020 ± 0.0029	0.00 ± 0.00015
Cesium (Cs)	0.0097 ± 0.0095	0.022 ± 0.031	0.010 ± 0.014	0.058 ± 0.0010	0.00 ± 0.00056	0.00 ± 0.00060	0.00 ± 0.00044	0.00 ± 0.00041
Barium (Ba)	0.00 ± 0.00059	0.00 ± 0.00077	0.00 ± 0.00086	0.00 ± 0.00089	0.00 ± 0.00042	0.00 ± 0.00046	0.00 ± 0.00034	0.00 ± 0.00031
Lanthanum (La)	0.015 ± 0.026	0.065 ± 0.025	0.055 ± 0.0026	0.00 ± 0.0015	0.042 ± 0.044	0.0053 ± 0.0075	0.019 ± 0.028	0.036 ± 0.021
Wolfram (W)	0.0034 ± 0.0059	0.0082 ± 0.0061	0.00 ± 0.00033	0.00 ± 0.00029	0.0037 ± 0.0018	0.0034 ± 0.0049	0.0019 ± 0.0028	0.00 ± 0.00012
Gold (Au)	0.00 ± 0.000066	0.0032 ± 0.0045	0.00 ± 0.000098	0.00 ± 0.000085	0.00062 ± 0.00088	0.00 ± 0.000051	0.00022 ± 0.00031	0.0012 ± 0.0017
Mercury (Hg)	0.00034 ± 0.00059	0.0014 ± 0.0020	0.00 ± 0.000052	0.00 ± 0.000045	0.00020 ± 0.00028	0.0014 ± 0.0020	0.00 ± 0.000020	0.00024 ± 0.00033
Lead (Pb)	0.00 ± 0.000066	0.0010 ± 0.0015	0.00 ± 0.000098	0.0036 ± 0.000085	0.0015 ± 0.0021	0.0014 ± 0.000962	0.00076 ± 0.0011	0.0012 ± 0.0017
Uranium (U)	0.0050 ± 0.0044	0.0028 ± 0.0027	0.0011 ± 0.0015	0.0035 ± 0.00015	0.0034 ± 0.0044	0.00 ± 0.000092	0.0026 ± 0.0037	0.00 ± 0.000062

Table 1 (cont'd)

	Average ± Standard Deviation of Percent $PM_{2.5}$ Mass							
	Subtropical				Tropical			
	Everglades National Park, Florida (FL2)				Borneo, Malaysia			
Aging Time	2 days		7 days		2 days		7 days	
	Fresh 2	Aged 2	Fresh 7	Aged 7	Fresh 2	Aged 2	Fresh 7	Aged 7
Peat IDs in the average[c]	PEAT010, PEAT011, PEAT012, PEAT015		PEAT016, PEAT017, PEAT018		PEAT036, PEAT038		PEAT039, PEAT041	
Nitric Acid (HNO_3)	0.38 ± 0.13	0.47 ± 0.37	0.28 ± 0.042	0.25 ± 0.13	0.20 ± 0.0080	0.26 ± 0.040	0.23 ± 0.18	0.17 ± 0.026
Ammonia (NH_3)	51.12 ± 27.44	14.37 ± 5.54	63.89 ± 25.088	4.79 ± 0.60	20.34 ± 0.0030	9.67 ± 2.25	25.50 ± 1.98	4.88 ± 1.76
Water-Soluble Sodium (Na^+)	0.047 ± 0.018	0.056 ± 0.016	0.030 ± 0.017	0.022 ± 0.0063	0.017 ± 0.0090	0.033 ± 0.023	0.018 ± 0.011	0.032 ± 0.017
Water-Soluble Potassium (K^+)	1.11 ± 2.15	na[d]	0.025 ± 0.017	na[d]	0.031 ± 0.028	na[d]	0.048 ± 0.035	na[d]
Chloride (Cl^-)	0.26 ± 0.072	0.21 ± 0.12	0.22 ± 0.018	0.086 ± 0.024	0.11 ± 0.024	0.10 ± 0.026	0.16 ± 0.073	0.10 ± 0.00025
Nitrite (NO_2^-)	0.058 ± 0.098	0.0020 ± 0.0031	0.00085 ± 0.0015	0.0023 ± 0.00072	0.00 ± 0.00025	0.00098 ± 0.0014	0.00 ± 0.00030	0.015 ± 0.019
Nitrate (NO_3^-)	0.27 ± 0.26	2.64 ± 0.76	0.14 ± 0.097	7.76 ± 1.029	0.087 ± 0.046	0.91 ± 0.22	0.13 ± 0.12	4.69 ± 1.34
Sulfate ($SO_4^{=}$)	1.40 ± 1.89	1.33 ± 0.69	0.34 ± 0.022	1.99 ± 0.28	0.17 ± 0.024	0.56 ± 0.18	0.13 ± 0.062	1.96 ± 0.071
Ammonium (NH_4^+)	0.0013 ± 0.0015	0.37 ± 0.60	0.0036 ± 0.00092	4.55 ± 0.57	0.0017 ± 0.0011	0.83 ± 0.086	0.0027 ± 0.00048	4.74 ± 0.77
OC1 (140°C)	11.40 ± 1.25	7.017 ± 3.95	18.049 ± 2.22	4.012 ± 0.89	16.033 ± 2.088	6.37 ± 3.36	15.20 ± 1.21	5.83 ± 3.45
OC2 (280°C)	23.86 ± 6.033	16.25 ± 3.60	24.53 ± 3.41	12.12 ± 0.86	22.44 ± 1.91	18.78 ± 4.51	23.41 ± 0.25	12.14 ± 2.71
OC3 (480°C)	23.70 ± 7.73	21.13 ± 3.73	23.33 ± 2.32	17.83 ± 3.95	25.52 ± 2.55	28.64 ± 4.52	26.24 ± 1.16	20.82 ± 3.30
OC4 (580°C)	9.010 ± 3.51	8.53 ± 2.94	6.15 ± 0.95	5.65 ± 1.23	4.37 ± 0.18	8.32 ± 1.099	5.56 ± 1.40	5.59 ± 0.82
Pyrolized Carbon (OP)	10.73 ± 2.31	9.89 ± 3.86	13.036 ± 1.020	12.30 ± 1.22	10.74 ± 0.66	12.56 ± 4.73	10.35 ± 0.11	13.15 ± 2.69
Organic Carbon (OC)[g]	78.69 ± 18.69	62.82 ± 14.029	85.086 ± 5.65	51.90 ± 3.86	79.10 ± 3.21	74.66 ± 18.22	80.76 ± 0.99	57.53 ± 11.32
EC1 (580°C)	8.59 ± 4.065	8.56 ± 2.77	7.53 ± 1.22	11.035 ± 1.98	6.43 ± 0.48	8.57 ± 3.59	6.85 ± 0.21	9.13 ± 0.94
EC2 (740°C)	6.54 ± 2.76	3.42 ± 3.41	7.59 ± 1.66	3.35 ± 2.14	5.12 ± 0.25	6.18 ± 1.64	5.14 ± 0.16	4.69 ± 0.81
EC3 (840°C)	0.00 ± 0.00029	0.00 ± 0.00026	0.00 ± 0.00027	0.00 ± 0.00016	0.00 ± 0.00017	0.00 ± 0.00020	0.00 ± 0.00020	0.00 ± 0.00018
Elemental Carbon (EC)[g]	4.40 ± 1.51	2.084 ± 0.52	2.084 ± 1.81	2.092 ± 1.11	0.82 ± 0.074	2.19 ± 0.50	1.63 ± 0.16	0.67 ± 0.94
Total Carbon (TC)	83.090 ± 19.45	64.90 ± 14.48	87.17 ± 7.38	54.00 ± 4.57	79.92 ± 3.29	76.86 ± 18.72	82.39 ± 1.14	58.20 ± 10.38
Water-Soluble OC (WSOC)	31.71 ± 8.36	28.89 ± 4.08	34.33 ± 4.82	23.28 ± 2.80	14.62 ± 0.92	22.88 ± 2.33	17.15 ± 2.80	22.90 ± 0.76
Formic acid (CH_2O_2)	0.14 ± 0.17	0.30 ± 0.052	0.054 ± 0.020	0.42 ± 0.23	0.10 ± 0.014	0.26 ± 0.049	0.13 ± 0.019	0.42 ± 0.10
Acetic acid ($C_2H_4O_2$)	0.33 ± 0.25	0.38 ± 0.063	0.22 ± 0.12	0.35 ± 0.13	0.29 ± 0.0081	0.59 ± 0.24	0.58 ± 0.075	0.56 ± 0.018
Oxalic acid ($C_2H_2O_4$)	0.11 ± 0.058	0.94 ± 0.22	0.082 ± 0.029	3.14 ± 0.56	0.26 ± 0.12	1.14 ± 0.21	0.43 ± 0.22	3.36 ± 0.28
Propionic acid ($C_3H_5O_2$)	0.0064 ± 0.013	0.00 ± 0.00018	0.018 ± 0.031	0.012 ± 0.020	0.045 ± 0.019	0.0095 ± 0.013	0.012 ± 0.017	0.066 ± 0.094
Levoglucosan ($C_6H_{10}O_5$)	1.08 ± 1.34	0.86 ± 1.073	2.22 ± 0.66	0.62 ± 0.81	2.52 ± 0.016	2.28 ± 0.99	4.38 ± 0.50	2.53 ± 0.19
Mannosan ($C_6H_{10}O_5$)	0.00 ± 0.00045	0.00 ± 0.00039	0.056 ± 0.097	0.24 ± 0.42	0.00 ± 0.00027	0.00 ± 0.00030	0.19 ± 0.26	0.082 ± 0.12
Galactose/Maltitol ($C_6H_{12}O_6$/$C_{12}H_{24}O_{11}$)	0.00 ± 0.00023	0.00 ± 0.00020	0.00 ± 0.00021	0.00 ± 0.00012	0.00 ± 0.00014	0.13 ± 0.18	0.00 ± 0.00017	0.00 ± 0.00014
Glycerol ($C_3H_8O_3$)	0.00 ± 0.0000041	0.00 ± 0.0000036	0.00 ± 0.0000038	0.00 ± 0.0000022	0.00 ± 0.0000025	0.00 ± 0.0000028	0.00 ± 0.0000030	0.00 ± 0.0000024
Mannitol ($C_6H_{14}O_6$)	0.00 ± 0.000083	0.00 ± 0.000072	0.00 ± 0.000075	0.00 ± 0.000043	0.011 ± 0.016	0.00 ± 0.000055	0.00 ± 0.000060	0.00 ± 0.000049
Aluminum (Al)	0.043 ± 0.86	0.070 ± 1.20	0.00024 ± 0.0041	0.00 ± 0.026[c]	0.033 ± 0.47	0.085 ± 0.030	0.045 ± 0.64	0.15 ± 0.030
Silicon (Si)	0.027 ± 0.52	0.26 ± 3.92	0.00 ± 0.00059	0.46 ± 0.31	0.012 ± 0.17	0.082 ± 0.0036	0.00 ± 0.00043	0.69 ± 0.0043
Phosphorous (P)	0.00 ± 0.00013	0.00 ± 0.00011	0.00 ± 0.00012	0.00 ± 0.000061	0.00 ± 0.000072	0.00 ± 0.000071	0.00 ± 0.000086	0.00 ± 0.000071

Table 1 (cont'd)

	Average ± Standard Deviation of Percent $PM_{2.5}$ Mass							
	Subtropical				Tropical			
	Everglades National Park, Florida (FL2)				Borneo, Malaysia			
Aging Time	2 days		7 days		2 days		7 days	
	Fresh 2	Aged 2	Fresh 7	Aged 7	Fresh 2	Aged 2	Fresh 7	Aged 7
Peat IDs in the average[c]	PEAT010, PEAT011, PEAT012, PEAT015		PEAT016, PEAT017, PEAT018		PEAT036, PEAT038		PEAT039, PEAT041	
Sulfur (S)	0.39 ± 0.23	0.59 ± 0.27	0.42 ± 0.066	1.12 ± 0.094	0.11 ± 0.12	0.39 ± 0.00013	0.029 ± 0.0022	0.83 ± 0.00026
Chlorine (Cl)	0.21 ± 0.088	0.065 ± 0.029	0.24 ± 0.024	0.038 ± 0.011	0.074 ± 0.0012	0.067 ± 0.000035	0.085 ± 0.0038	0.047 ± 0.000030
Potassium (K)	0.034 ± 0.015	0.51 ± 0.37	0.018 ± 0.014	0.22 ± 0.052	0.051 ± 0.049	0.084 ± 0.00010	0.028 ± 0.017	0.017 ± 0.00010
Calcium (Ca)	0.00 ± 0.00067	0.0081 ± 0.016	0.00 ± 0.00061	0.010 ± 0.014	0.0058 ± 0.0082	0.00 ± 0.00037	0.00 ± 0.00046	0.023 ± 0.00038
Scandium (Sc)	0.00 ± 0.0030	0.00 ± 0.0026	0.00 ± 0.0027	0.00 ± 0.0014	0.00 ± 0.0017	0.00 ± 0.0017	0.00 ± 0.0020	0.00 ± 0.0017
Titanium (Ti)	0.0061 ± 0.0079	0.017 ± 0.035	0.00 ± 0.000098	0.00 ± 0.000051	0.0073 ± 0.010	0.00 ± 0.000059	0.0066 ± 0.0094	0.00 ± 0.000059
Vanadium (V)	0.0010 ± 0.0020	0.00 ± 0.000017	0.00 ± 0.000018	0.0065 ± 0.0092	0.00 ± 0.000011	0.00 ± 0.000011	0.00 ± 0.000014	0.00 ± 0.000011
Chromium (Cr)	0.00 ± 0.000066	0.00056 ± 0.0011	0.00 ± 0.000061	0.00016 ± 0.00023	0.00 ± 0.000038	0.00 ± 0.000037	0.0026 ± 0.0037	0.00 ± 0.000037
Manganese (Mn)	0.0032 ± 0.0064	0.0051 ± 0.0050	0.0017 ± 0.0015	0.0034 ± 0.0043	0.0055 ± 0.0026	0.0075 ± 0.00013	0.0088 ± 0.00010	0.0046 ± 0.00013
Iron (Fe)	0.023 ± 0.021	0.065 ± 0.034	0.020 ± 0.016	0.091 ± 0.096	0.074 ± 0.0078	0.074 ± 0.00023	0.045 ± 0.020	0.043 ± 0.00023
Cobalt (Co)	0.000055 ± 0.00011	0.000045 ± 0.000090	0.00024 ± 0.00041	0.00 ± 0.0000064	0.00 ± 0.0000075	0.00061 ± 0.0000074	0.00 ± 0.0000090	0.000087 ± 0.0000074
Nickel (Ni)	0.00026 ± 0.00042	0.00 ± 0.000029	0.00 ± 0.000031	0.00038 ± 0.00054	0.00064 ± 0.00091	0.00 ± 0.000019	0.0034 ± 0.0014	0.00 ± 0.000019
Copper (Cu)	0.010 ± 0.0080	0.21 ± 0.23	0.0033 ± 0.0036	0.021 ± 0.0024	0.0054 ± 0.0042	0.0075 ± 0.00012	0.0091 ± 0.0013	0.0017 ± 0.00012
Zinc (Zn)	0.0039 ± 0.0011	0.0091 ± 0.0039	0.0021 ± 0.0019	0.023 ± 0.027	0.0043 ± 0.0037	0.00 ± 0.000063	0.0034 ± 0.0018	0.00 ± 0.000063
Arsenic (As)	0.00059 ± 0.00069	0.0013 ± 0.0020	0.00 ± 0.000049	0.00 ± 0.000025	0.00 ± 0.000030	0.00 ± 0.000030	0.00 ± 0.000036	0.0028 ± 0.000030
Selenium (Se)	0.0011 ± 0.0014	0.0023 ± 0.0018	0.0037 ± 0.0025	0.00016 ± 0.00023	0.0019 ± 0.0010	0.00 ± 0.000052	0.00086 ± 0.0012	0.00 ± 0.000052
Bromine (Br)	0.030 ± 0.015	0.0090 ± 0.0049	0.022 ± 0.0072	0.0088 ± 0.0036	0.011 ± 0.0015	0.012 ± 0.000015	0.012 ± 0.0026	0.0044 ± 0.000015
Rubidium (Rb)	0.00038 ± 0.00077	0.0015 ± 0.0014	0.0015 ± 0.0026	0.00 ± 0.000016	0.00039 ± 0.00056	0.00035 ± 0.000019	0.00 ± 0.000023	0.0017 ± 0.000019
Strontium (Sr)	0.0051 ± 0.0012	0.0044 ± 0.0023	0.0055 ± 0.0063	0.0033 ± 0.0022	0.0028 ± 0.00026	0.0021 ± 0.000019	0.0070 ± 0.00099	0.0029 ± 0.000019
Yttrium (Y)	0.0043 ± 0.0051	0.0021 ± 0.0034	0.0014 ± 0.00060	0.00 ± 0.0000016	0.0018 ± 0.0023	0.0032 ± 0.000019	0.0018 ± 0.0016	0.0027 ± 0.000019
Zirconium (Zr)	0.0041 ± 0.0038	0.0049 ± 0.0066	0.0040 ± 0.0069	0.0051 ± 0.0039	0.0048 ± 0.00038	0.0016 ± 0.000071	0.00052 ± 0.00074	0.00 ± 0.000071
Niobium (Nb)	0.0016 ± 0.0022	0.00080 ± 0.0013	0.0019 ± 0.0026	0.00 ± 0.000029	0.00095 ± 0.0014	0.00 ± 0.000034	0.0021 ± 0.0030	0.00026 ± 0.000034
Molybdenum (Mo)	0.0022 ± 0.0021	0.0013 ± 0.0017	0.0012 ± 0.0022	0.00081 ± 0.0011	0.00071 ± 0.0010	0.00 ± 0.000071	0.0044 ± 0.00018	0.0032 ± 0.000071
Silver (Ag)	0.0014 ± 0.0029	0.00 ± 0.00014	0.00 ± 0.00015	0.00 ± 0.000076	0.0025 ± 0.0035	0.00 ± 0.000089	0.0026 ± 0.0037	0.00 ± 0.000089
Cadmium (Cd)	0.00 ± 0.00022	0.00 ± 0.00019	0.0075 ± 0.013	0.0095 ± 0.0060	0.00044 ± 0.00063	0.00 ± 0.00012	0.00 ± 0.00015	0.00 ± 0.00012
Indium (In)	0.0069 ± 0.0049	0.0023 ± 0.0046	0.0054 ± 0.0093	0.0012 ± 0.0017	0.0048 ± 0.0067	0.0013 ± 0.000085	0.00087 ± 0.0012	0.00 ± 0.000085
Tin (Sn)	0.0061 ± 0.0072	0.0058 ± 0.012	0.0061 ± 0.0058	0.0068 ± 0.0096	0.0022 ± 0.0031	0.013 ± 0.00016	0.0038 ± 0.0054	0.012 ± 0.00016
Antimony (Sb)	0.00028 ± 0.00056	0.00040 ± 0.00052	0.00033 ± 0.00057	0.00050 ± 0.00071	0.00 ± 0.00024	0.0039 ± 0.00023	0.011 ± 0.0097	0.00 ± 0.00023
Cesium (Cs)	0.000088 ± 0.00018	0.028 ± 0.037	0.037 ± 0.064	0.00 ± 0.00057	0.028 ± 0.031	0.020 ± 0.00066	0.0077 ± 0.011	0.00 ± 0.00066
Barium (Ba)	0.00 ± 0.00088	0.00 ± 0.00085	0.00 ± 0.00081	0.00 ± 0.00044	0.00 ± 0.00050	0.00 ± 0.00050	0.00 ± 0.00060	0.00 ± 0.00050
Lanthanum (La)	0.054 ± 0.039	0.033 ± 0.039	0.036 ± 0.039	0.0049 ± 0.0070	0.041 ± 0.058	0.00 ± 0.00097	0.018 ± 0.025	0.080 ± 0.00097
Wolfram (W)	0.010 ± 0.012	0.0030 ± 0.0051	0.0080 ± 0.014	0.00 ± 0.00016	0.00 ± 0.00019	0.0058 ± 0.00019	0.00 ± 0.00023	0.00 ± 0.00019
Gold (Au)	0.0012 ± 0.0013	0.00082 ± 0.0016	0.0046 ± 0.0045	0.00033 ± 0.00047	0.00051 ± 0.00072	0.00 ± 0.000056	0.00041 ± 0.00058	0.00 ± 0.000056
Mercury (Hg)	0.00035 ± 0.00070	0.00091 ± 0.0015	0.00 ± 0.000049	0.00 ± 0.000025	0.00 ± 0.000030	0.00 ± 0.000030	0.00041 ± 0.00058	0.000087± 0.000030
Lead (Pb)	0.0017 ± 0.0035	0.0012 ± 0.0024	0.0018 ± 0.0031	0.0028 ± 0.0026	0.0031 ± 0.0044	0.00052 ± 0.000056	0.0016 ± 0.0022	0.00 ± 0.000056
Uranium (U)	0.0027 ± 0.0031	0.0023 ± 0.0026	0.0044 ± 0.0077	0.0017 ± 0.0023	0.00 ± 0.00010	0.0033 ± 0.00010	0.0057 ± 0.00076	0.0062 ± 0.00010

[a]Analytical uncertainties are used for species below the minimum detection limit, mostly for carbohydrate species and elements with an average concentration of 0.00

[b]Only one sample was analyzed for elements by x-ray fluorescence with abundance and measurement uncertainty

[c]Peat ID code, detailed operation parameters are reported in Watson et al. (2019)

[d]Data not available; water-soluble K^+ data were contaminated for aged samples due to the use of potassium iodide denuder downstream of the oxidation flow reactor

[e]WSOC measures from Peat sample ID PEAT028 was invalidated due to a crack in the test tube. Therefore, only two measurements are used to calculate the average and standard deviation.

[f]Data not available due to the invalidated citric acid impregnated filter sample

[g]The carbon analysis follows the IMPROVE_A thermal/optical reflectance protocol (Chow et al., 2007) that is applied in long-term U.S. non-urban IMPROVE and urban Chemical Speciation Network. Organic carbon (OC) is the sum of OC1+OC2+OC3+OC4 plus pyrolized carbon (OP). Elemental carbon (EC) is the sum of EC1+EC2+EC3 minus OP. Total carbon is the sum of OC and EC. Since a large fraction of OP (7–13 %) are found in smoldering peat combustion emissions--indicative of higher molecular-weight compounds that are likely to char, the resulting EC are lower than the individual EC fraction after OP correction.

Table 2. Equivalence measures[a] for comparison of $PM_{2.5}$ peat source profiles.

A All Fresh (Profile #1) vs. All Aged (Profile #2) by Biome (group comparison of fresh and aged samples)

Peat region[b]	Peats Included	n1[c]	n2[c]	Percent Distribution				Correlation Coefficient	*P*-value[d]
				< 1 σ	1 - 2 σ	2 - 3 σ	> 3 σ		
Boreal	Russia + Siberia	12	12	93.60%	5.60%	0.80%	0.00%	0.995	0.00012
Boreal + Temperate	Russia + Siberia + Alaska	17	17	95.20%	4.80%	0.00%	0.00%	0.996	0.00010
Temperate	Alaska	5	5	96.00%	4.00%	0.00%	0.00%	0.997	0.00008
Subtropical 1	Florida-1 (FL1)	4	4	77.60%	14.40%	5.60%	2.40%	0.993	0.94570
Subtropical 2	Florida-2 (FL2)	7	7	77.78%	21.43%	0.79%	0.00%	0.986	0.00001
Subtropical 1 + Temperate	Florida-1 + Alaska	9	9	96.83%	3.17%	0.00%	0.00%	0.996	0.00073
Subtropical 2 + Temperate	Florida-2 + Alaska	12	12	81.75%	18.25%	0.00%	0.00%	0.992	0.00001
Tropical	Malaysia	4	4	78.57%	18.25%	1.59%	1.59%	0.994	0.00195
Subtropical 1 + Tropical	Florida-1 + Malaysia	8	8	83.33%	15.87%	0.00%	0.79%	0.995	0.01686
Subtropical 2 + Tropical	Florida-2 + Malaysia	11	11	80.16%	19.05%	0.79%	0.00%	0.991	0.00003

B Fresh 2 vs. Aged 2 by Biome (paired comparison for 2-day aging)

Peat region	Peats Included	n1	n2	Percent Distribution				Correlation Coefficient	*P*-value
				< 1 σ	1 - 2 σ	2 - 3 σ	> 3 σ		
Boreal	Russia + Siberia	6	6	94.40%	3.20%	2.40%	0.00%	0.997	0.00088
Boreal + Temperate	Russia + Siberia + Alaska	9	9	95.20%	4.00%	0.80%	0.00%	0.997	0.00237
Temperate	Alaska	3	3	86.40%	11.20%	0.80%	1.60%	0.997	0.02474
Subtropical 1	Florida-1	2	2	78.86%	13.82%	3.25%	4.07%	0.994	0.30785
Subtropical 2	Florida-2	4	4	86.51%	11.90%	0.79%	0.79%	0.992	0.00000
Subtropical 1 + Temperate	Florida-1 + Alaska	5	5	92.00%	7.20%	0.80%	0.00%	0.997	0.04329
Subtropical 2 + Temperate	Florida-2 + Alaska	7	7	95.24%	3.97%	0.00%	0.79%	0.996	0.00002
Tropical	Malaysia	2	2	80.00%	5.33%	5.33%	9.33%	0.996	0.95960
Subtropical 1 + Tropical	Florida-1 + Malaysia	4	4	88.89%	8.73%	1.59%	0.79%	0.996	0.62905
Subtropical 2 + Tropical	Florida-2 + Malaysia	6	6	93.65%	5.56%	0.00%	0.79%	0.995	0.00002

C Fresh 7 vs. Aged 7 by Biome (paired comparison for 7-day aging)

Peat region	Peats Included	n1	n2	Percent Distribution				Correlation Coefficient	*P*-value
				< 1 σ	1 - 2 σ	2 - 3 σ	> 3 σ		
Boreal	Russia + Siberia	6	6	76.00%	20.80%	1.60%	1.60%	0.992	0.00007
Boreal + Temperate	Russia + Siberia + Alaska	8	8	76.80%	20.00%	0.80%	2.40%	0.993	0.00003
Temperate	Alaska	2	2	64.86%	25.68%	2.70%	6.76%	0.993	0.00000
Subtropical 1	Florida-1	2	2	63.20%	13.60%	7.20%	16.00%	0.998	0.00027
Subtropical 2	Florida-2	3	3	66.67%	9.52%	3.17%	20.63%	0.975	0.00003
Subtropical 1 + Temperate	Florida-1 + Alaska	4	4	88.10%	7.94%	3.97%	0.00%	0.994	0.00004
Subtropical 2 + Temperate	Florida-2 + Alaska	5	5	73.02%	19.84%	3.97%	3.17%	0.984	0.00001
Tropical	Malaysia	2	2	41.33%	21.33%	24.00%	13.33%	0.989	0.00017
Subtropical 1 + Tropical	Florida-1 + Malaysia	4	4	72.22%	23.81%	0.79%	3.17%	0.993	0.00156
Subtropical 2 + Tropical	Florida-2 + Malaysia	5	5	73.02%	8.73%	1.59%	16.67%	0.983	0.00004

D Fresh 2 vs. Fresh 7 by Biome (comparison between different experiments for unaged fresh profiles)

Peat region	Peats Included	n1	n2	Percent Distribution				Correlation Coefficient	*P*-value
				< 1 σ	1 - 2 σ	2 - 3 σ	> 3 σ		
Boreal	Russia + Siberia	6	6	97.62%	2.38%	0.00%	0.00%	0.999	0.00004
Boreal + Temperate	Russia + Siberia + Alaska	9	8	100.00%	0.00%	0.00%	0.00%	0.999	0.00148
Temperate	Alaska	3	2	91.27%	6.35%	0.79%	1.59%	0.996	0.12876
Subtropical 1	Florida-1	2	2	90.32%	6.45%	1.61%	1.61%	0.999	0.00001
Subtropical 2	Florida-2	4	3	97.62%	1.59%	0.79%	0.00%	0.999	0.00032
Subtropical 1 + Temperate	Florida-1 + Alaska	5	4	99.21%	0.79%	0.00%	0.00%	0.998	0.00308
Subtropical 2 + Temperate	Florida-2 + Alaska	7	5	100.00%	0.00%	0.00%	0.00%	0.998	0.02743
Tropical	Malaysia	2	2	81.10%	10.24%	3.15%	5.51%	0.999	0.00006
Subtropical 1 + Tropical	Florida-1 + Malaysia	4	4	94.49%	4.72%	0.79%	0.00%	1.000	0.03537
Subtropical 2 + Tropical	Florida-2 + Malaysia	6	5	98.43%	1.57%	0.00%	0.00%	0.999	0.00013

E Aged 2 vs. Aged 7 by Biome (comparison between different experiments for the 2- and 7-day aging times)

Peat region	Peats Included	n1	n2	Percent Distribution				Correlation Coefficient	*P*-value
				< 1 σ	1 - 2 σ	2 - 3 σ	> 3 σ		
Boreal	Russia + Siberia	6	6	95.20%	3.20%	1.60%	0.00%	0.997	0.00018
Boreal + Temperate	Russia + Siberia + Alaska	9	8	94.40%	3.20%	1.60%	0.80%	0.998	0.00002
Temperate	Alaska	3	2	66.22%	27.03%	5.41%	1.35%	0.996	0.00000
Subtropical 1	Florida-1	2	2	83.20%	9.60%	1.60%	5.60%	1.000	0.00017
Subtropical 2	Florida-2	4	3	88.89%	8.73%	0.00%	2.38%	0.994	0.00298
Subtropical 1 + Temperate	Florida-1 + Alaska	5	4	94.44%	5.56%	0.00%	0.00%	0.999	0.00000
Subtropical 2 + Temperate	Florida-2 + Alaska	7	5	81.75%	16.67%	0.00%	1.59%	0.997	0.00003
Tropical	Malaysia	2	2	81.33%	13.33%	1.33%	4.00%	0.997	0.00002
Subtropical 1 + Tropical	Florida-1 + Malaysia	4	4	92.06%	7.14%	0.79%	0.00%	0.999	0.00002
Subtropical 2 + Tropical	Florida-2 + Malaysia	6	5	93.65%	3.97%	0.79%	1.59%	0.996	0.00035

[a]For the *t*-test, a cutoff probability level of 5% is selected; if $P < 0.05$, there is a 95% probability that the two profiles are different. For correlations, $r > 0.8$ suggests similar profiles, $0.5 < r < 0.8$ indicates a moderate similarity, and $r < 0.5$ denotes little or no similarity. The R/U ratio indicates the percentage of the >93 reported chemical abundances differ by more than an expected number of uncertainty intervals. The normal probability density function of 68%, 95.5%, and 99.7% for $\pm 1s$, $\pm 2s$, and $\pm 3s$, respectively, is used to evaluate the R/U ratios. The two profiles are considered to be similar, within the uncertainties of the chemical abundances when 80% of the R/U ratios are within $\pm 3s$, with $r > 0.8$ and $P > 0.05$. Species with R/U ratios $> 3s$ are further examined as these may be markers that further allow source contributions to be distinguishes by receptor measurements. They may also reflect the sampling and analysis artifacts that are not representative of the larger population of source profiles.

[b]Unless otherwise noted, Boreal represents Russia and Siberia regions, Temperate represents northern Alaska region, Subtropical is divided into Subtropical 1 for Putnam (FL1) and Subtropical 2 for Everglades (FL2) peats, and Tropical represents Island of Borneo, Malaysia region.

[c]n1 and n2 denote number of samples in comparison

[d]Student *t*-test *P*-values

Table 3. Organic carbon diagnostic ratios for different peat samples.

Peat Type	Atmospheric Aging time	OC/TC ± σ^a	OM[b]/OC ± σ^a	WSOC[c]/OC ± σ^a	(Levoglucosan/2.25)[d]/OC ± σ^a	(Oxalic acid/3.75)[e]/OC ± σ^a	(Levoglucosan/2.25)[d]/WSOC ± σ^a	(Oxalic acid/3.75)[e]/WSOC ± σ^a
Odintsovo, Russia	Fresh 2	0.97 ± 0.11	1.7 ± 0.15	0.64 ± 0.075	0.27 ± 0.066	0.00047 ± 0.00029	0.42 ± 0.10	0.00073 ± 0.00045
	Aged 2	0.97 ± 0.30	2.1 ± 0.46	0.70 ± 0.17	0.24 ± 0.10	0.0057 ± 0.0017	0.35 ± 0.13	0.0082 ± 0.0019
	Fresh 7	0.97 ± 0.12	1.6 ± 0.14	0.59 ± 0.065	0.28 ± 0.030	0.0012 ± 0.001	0.48 ± 0.040	0.0021 ± 0.0017
	Aged 7	0.95 ± 0.16	2.2 ± 0.26	0.71 ± 0.18	0.21 ± 0.051	0.019 ± 0.0055	0.30 ± 0.089	0.026 ± 0.0090
Pskov, Siberia	Fresh 2	0.96 ± 0.12	1.3 ± 0.12	0.32 ± 0.039	0.04 ± 0.016	0.00023 ± 0.000050	0.12 ± 0.049	0.00069 ± 0.00015
	Aged 2	0.96 ± 0.26	1.4 ± 0.27	0.44 ± 0.13	0.027 ± 0.0066	0.0051 ± 0.0021	0.063 ± 0.017	0.012 ± 0.0050
	Fresh 7	0.99 ± 0.17	1.2 ± 0.14	0.40 ± 0.046	0.051 ± 0.013	0.00025 ± 0.000067	0.13 ± 0.055	0.00063 ± 0.00015
	Aged 7	0.96 ± 0.14	1.5 ± 0.18	0.56 ± 0.17	0.031 ± 0.0043	0.019 ± 0.0073	0.057 ± 0.018	0.035 ± 0.016
Northern Alaska, USA	Fresh 2	0.97 ± 0.12	1.3 ± 0.10	0.38 ± 0.12	0.10 ± 0.047	0.00013 ± 0.00010	0.27 ± 0.15	0.00035 ± 0.00028
	Aged 2	0.97 ± 0.17	1.4 ± 0.18	0.40 ± 0.075	0.11 ± 0.025	0.0033 ± 0.00073	0.27 ± 0.063	0.0080 ± 0.0018
	Fresh 7	0.95 ± 0.38	1.4 ± 0.39	0.45 ± 0.20	0.061 ± 0.019	0.00016 ± 0.00023	0.14 ± 0.052	0.00037 ± 0.00053
	Aged 7	0.96 ± 0.35	1.8 ± 0.44	0.55 ± 0.16	0.046 ± 0.029	0.018 ± 0.0053	0.084 ± 0.052	0.034 ± 0.0076
Putnam County Lakebed, Florida, USA (FL1)	Fresh 2	0.95 ± 0.19	1.3 ± 0.18	0.27 ± 0.074	0.02 ± 0.0026	0.00019 ± 0.00026	0.072 ± 0.017	0.00068 ± 0.0010
	Aged 2	0.97 ± 0.10	1.4 ± 0.10	0.32 ± 0.067	0.018 ± 0.0013	0.0022 ± 0.0010	0.054 ± 0.011	0.0068 ± 0.0033
	Fresh 7	0.98 ± 0.094	1.5 ± 0.10	0.24 ± 0.024	0.021 ± 0.0021	na	0.085 ± 0.009	na
	Aged 7	0.98 ± 0.10	1.4 ± 0.11	0.34 ± 0.034	0.010 ± 0.0034	0.0044 ± 0.00082	0.029 ± 0.010	0.013 ± 0.0023
Everglades, Florida, USA (FL2)	Fresh 2	0.95 ± 0.32	1.2 ± 0.28	0.40 ± 0.14	0.0061 ± 0.0077	0.00036 ± 0.00021	0.015 ± 0.019	0.00089 ± 0.00054
	Aged 2	0.97 ± 0.31	1.5 ± 0.33	0.46 ± 0.12	0.0061 ± 0.0077	0.0044 ± 0.00082	0.013 ± 0.017	0.0086 ± 0.0024
	Fresh 7	0.98 ± 0.11	1.1 ± 0.079	0.40 ± 0.063	0.012 ± 0.0035	0.00026 ± 0.000092	0.029 ± 0.009	0.00064 ± 0.00024
	Aged 7	0.96 ± 0.11	1.6 ± 0.12	0.45 ± 0.063	0.0053 ± 0.007	0.016 ± 0.0031	0.012 ± 0.016	0.036 ± 0.0078
Borneo, Malaysia	Fresh 2	0.99 ± 0.057	1.2 ± 0.051	0.18 ± 0.014	0.014 ± 0.00058	0.00087 ± 0.00042	0.077 ± 0.005	0.0047 ± 0.0023
	Aged 2	0.97 ± 0.33	1.3 ± 0.31	0.31 ± 0.081	0.014 ± 0.0067	0.0041 ± 0.0012	0.044 ± 0.020	0.013 ± 0.0028
	Fresh 7	0.98 ± 0.018	1.2 ± 0.015	0.21 ± 0.035	0.024 ± 0.0027	0.0014 ± 0.00072	0.11 ± 0.023	0.0067 ± 0.0036
	Aged 7	0.99 ± 0.26	1.5 ± 0.29	0.40 ± 0.079	0.02 ± 0.0041	0.016 ± 0.0033	0.049 ± 0.0040	0.039 ± 0.0035

[a]Uncertainty associated with each ratio is calculated based on the square root of the individual uncertainties multiplied by the ratio (Bevington, 1969).

[b]OM (organic mass) is calculated by subtracting major ions (i.e., sum of NH_4^+, NO_3^-, and $SO_4^=$), crustal components (2.2Al + 2.49 Si + 1.63 Ca + 1.94 Ti + 2.42 Fe) and elemental carbon from $PM_{2.5}$ mass

[c]WSOC: water-soluble organic carbon

[d]Levoglucosan/2.25 represents carbon content in levoglucosan, based on the chemical composition $C_6H_{10}O_5$.

[e]Oxalic acid/3.75 represents carbon content in oxalic acid based on the chemical composition $C_2H_2O_4$.

(a) Upstream Filter Packs[a,b]

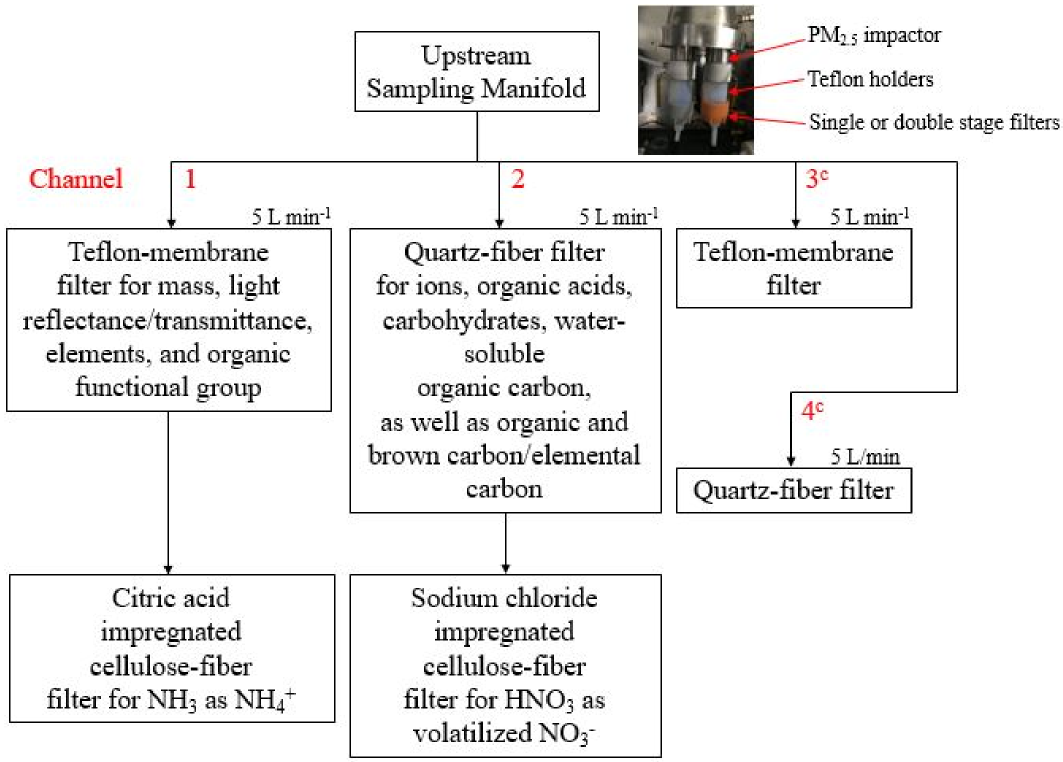

(b) Downstream Filter Packs[a,b]

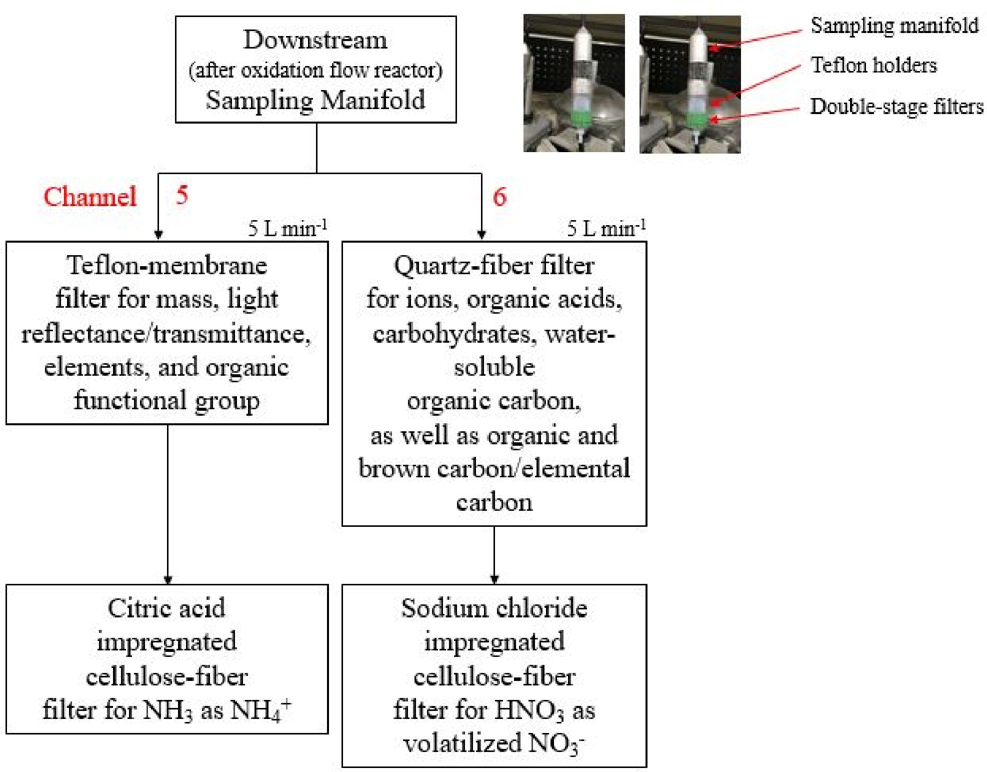

[a]The filter types are: 1) Teflon-membrane filter (Teflo©, 2 μm pore size, R2PJ047, Pall Life Sciences, Port Washington, NY, USA); 2) quartz-fiber filters (Tissuquartz, 2500 QAT-UP, Pall Life Sciences); and 3) citric acid and sodium chloride impregnated cellulose-fiber filters (31ET, Whatman Labware Products, St. Louis, MO, USA).

[b]Analyses include: 1) mass by gravimetry (Model XP6 microbalance, Mettler-Toledo, Columbus, OH, USA); 2) light reflectance/transmittance by UV/Vis spectrometry (Lambda35, Perkin Elmer, Waltham, MA, USA); 3) multiple elements by energy-dispersive x-ray fluorescence (XRF) (Epsilon 5 PANalytical, Westborough, MA, USA); 4) four anions (chloride [Cl^-], nitrite [NO_2^-], nitrate [NO_3^-], and sulfate [$SO_4^{=}$]); three cations (water-soluble sodium [Na^+], potassium [K^+], and ammonium [NH_4^+]); and ten organic acids (i.e., formic acid, acetic acid, lactic acid, methanesulfonic acid, oxalic acid, propionic acid, succinic acid, maleic acid, malonic acid, and glutaric acid) by ion chromatography (IC) with conductivity detector (Dionex Model ICS-5000+, Thermo Scientific, Waltham, MA, USA); 5) 17 carbohydrates (i.e., levoglucosan, mannosan, galactosan, glycerol, 2-methylerythritol, arabitol, mannitol, xylitol, erythritol, adonitol, inositol, glucose, galactose, arabinose, fructose, sucrose, and trehalose) by IC with pulsed amperometric detector (Dionex Model ICS3000, Thermo Scientific, Waltham, MA, USA); 6) water-soluble organic carbon (WSOC) by total organic carbon analyzer with non-dispersive infrared (NDIR) detector (Shimadzu Corporation, Kyoto, Japan); 7) organic functional groups by Fourier-Transform Infrared (FTIR) spectroscopy (VERTEX 70, Bruker, Billerica, MA, USA); and 8) organic, elemental, and brown carbon (OC, EC, and BrC) by multiwavelength thermal/optical carbon analyzer (DRI Model 2015, Magee Scientific, Berkeley, CA, USA).

[c]Teflon-membrane filter samples from Channel 3 are to be analyzed for additional organic nitrogen speciation using Fourier transform-ion cyclotron resonance mass spectrometry (FT-ICR-MS) at the Michigan Technological University. Quartz-fiber filter samples from Channel 4 are to be analyzed for polar and non-polar organics at the Hong Kong Premium Services and Research Laboratory.

Figure 1. Filter pack sampling configurations for upstream and downstream channels of the oxidation flow reactor.

Two-day aging	Seven-day aging

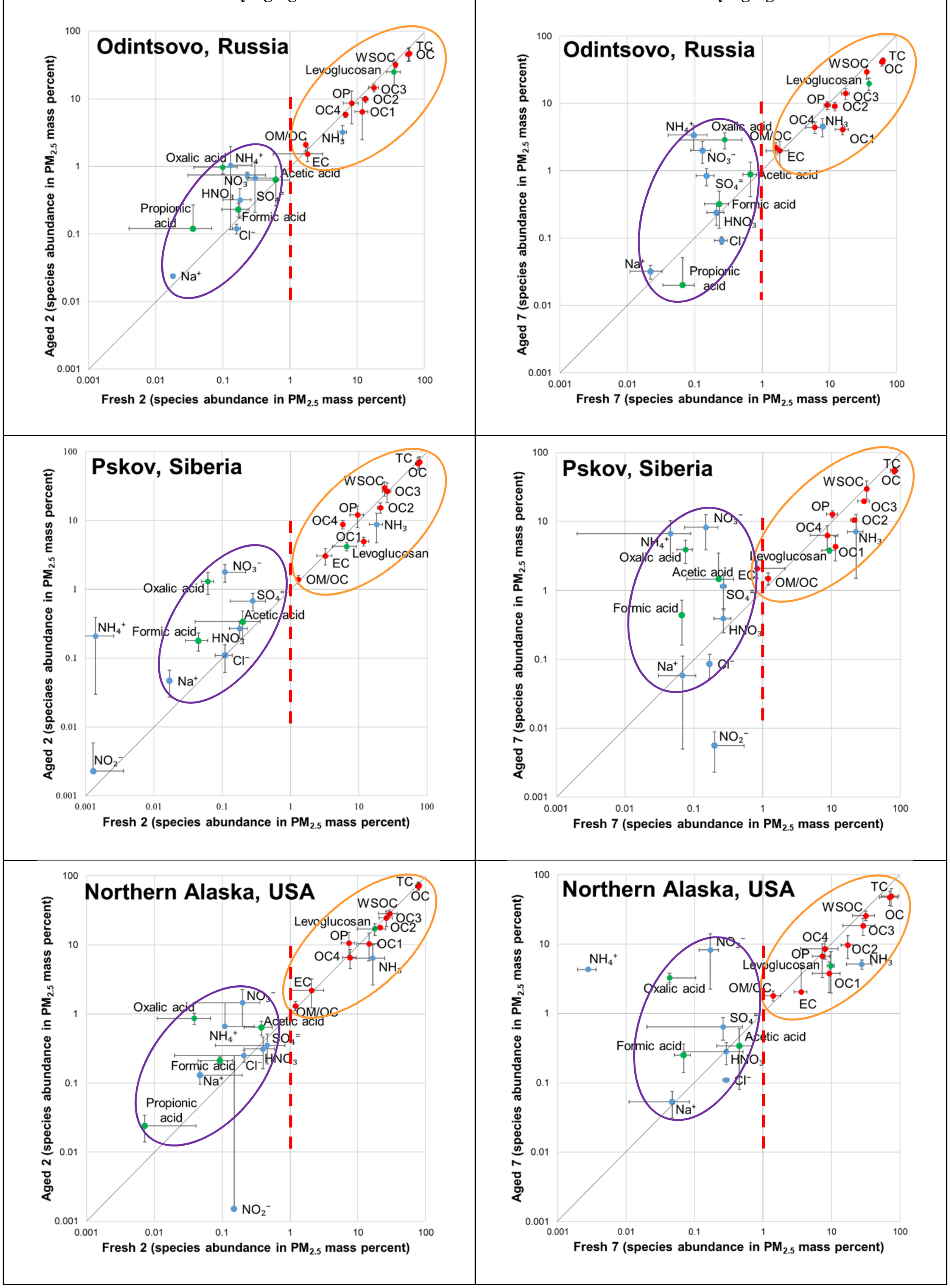

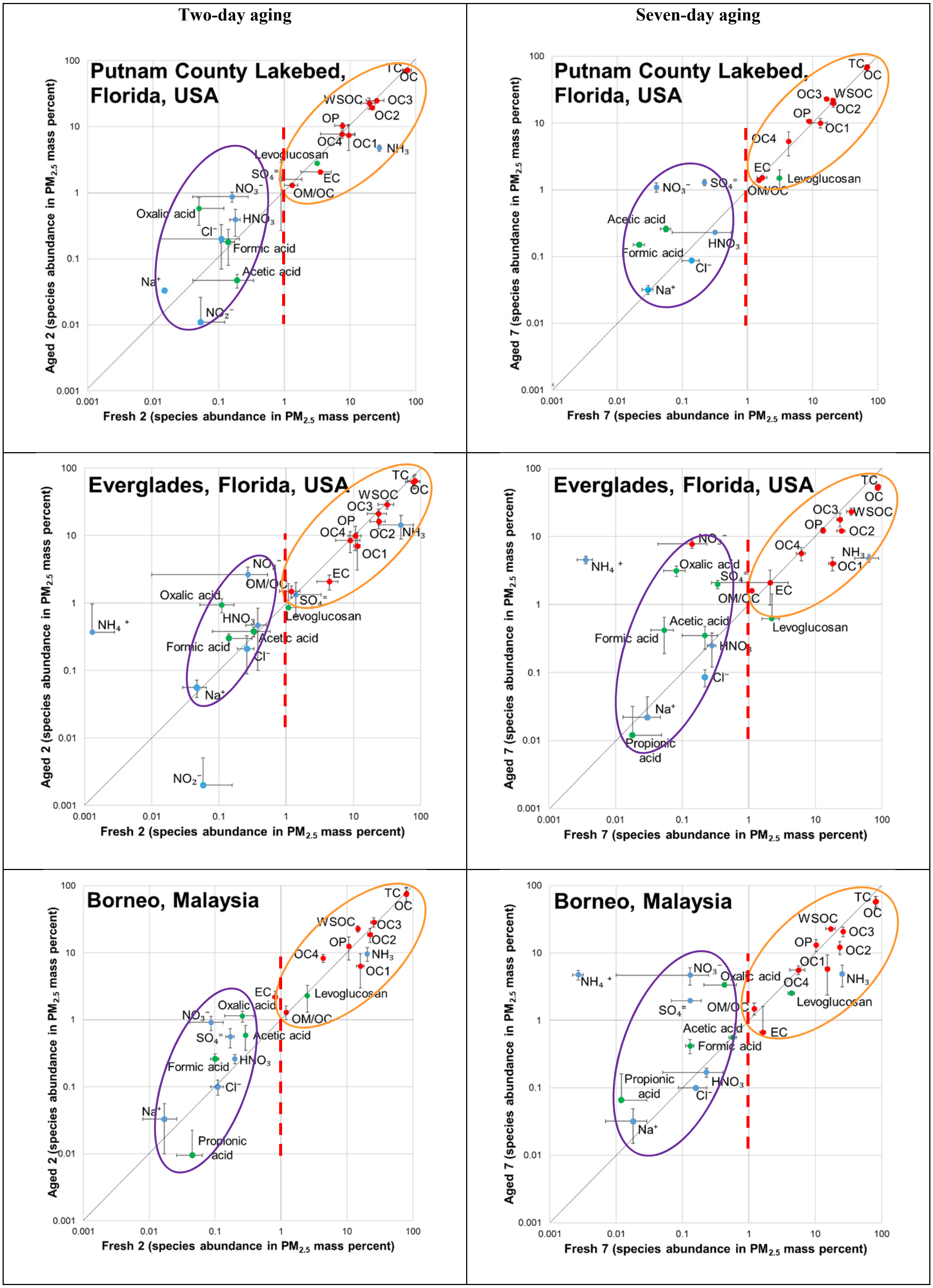

Two-day aging
Seven-day aging
Putnam County Lakebed, Florida, USA
Everglades, Florida, USA
Borneo, Malaysia
Aged 2 (species abundance in PM2.5 mass percent)
Fresh 2 (species abundance in PM2.5 mass percent)
Aged 7 (species abundance in PM2.5 mass percent)
Fresh 7 (species abundance in PM2.5 mass percent)
TC
OC
WSOC
OC1
OC2
OC3
OC4
OP
EC
OM/OC
NH3
NH4+
Levoglucosan
SO4=
NO3−
NO2−
HNO3
Cl−
Na+
Oxalic acid
Formic acid
Acetic acid
Propionic acid
0.001
0.01
0.1
1
10
100

Figure 2. Comparison between fresh and aged profile chemical abundances for each of the six types of peat with 2- and 7-day aging times. Standard deviations associated with averages in x and y axes are also shown. Vertical dashlines (red) on 1 % in x-axis intended to delineate the two distinguished clusters: centered around 0.1 % for reactive/ionic species and centered around 10 % for carbon compounds.

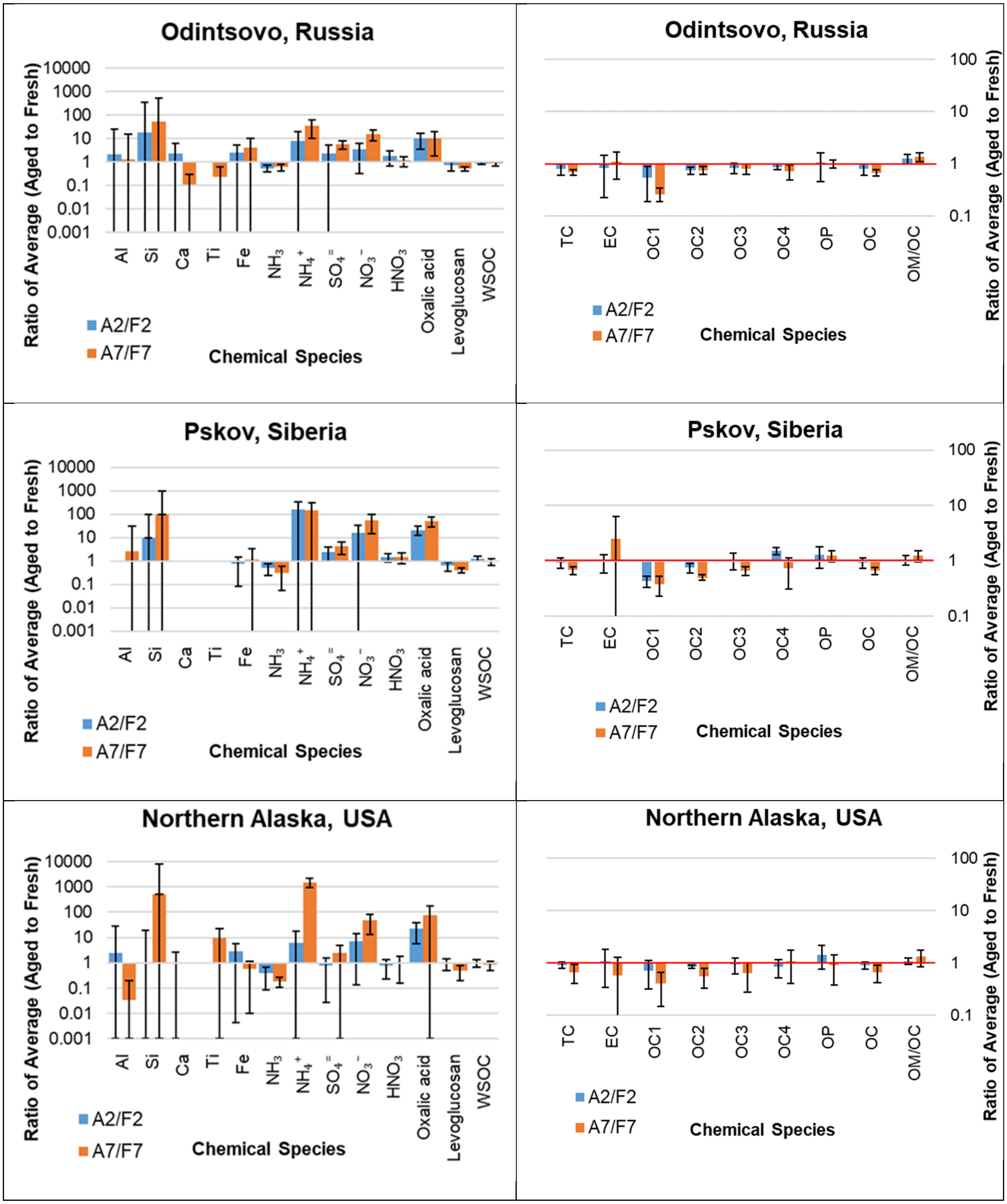
Odintsovo, Russia
Ratio of Average (Aged to Fresh)
10000
1000
100
10
1
0.1
0.01
0.001
Al
Si
Ca
Ti
Fe
NH_3
NH_4^+
$SO_4^=$
NO_3^-
HNO_3
Oxalic acid
Levoglucosan
WSOC
A2/F2
A7/F7
Chemical Species
Odintsovo, Russia
100
10
1
0.1
TC
EC
OC1
OC2
OC3
OC4
OP
OC
OM/OC
A2/F2
A7/F7
Chemical Species
Ratio of Average (Aged to Fresh)
Pskov, Siberia
Ratio of Average (Aged to Fresh)
A2/F2
A7/F7
Chemical Species
Pskov, Siberia
A2/F2
A7/F7
Chemical Species
Ratio of Average (Aged to Fresh)
Northern Alaska, USA
Ratio of Average (Aged to Fresh)
A2/F2
A7/F7
Chemical Species
Northern Alaska, USA
A2/F2
A7/F7
Chemical Species
Ratio of Average (Aged to Fresh)

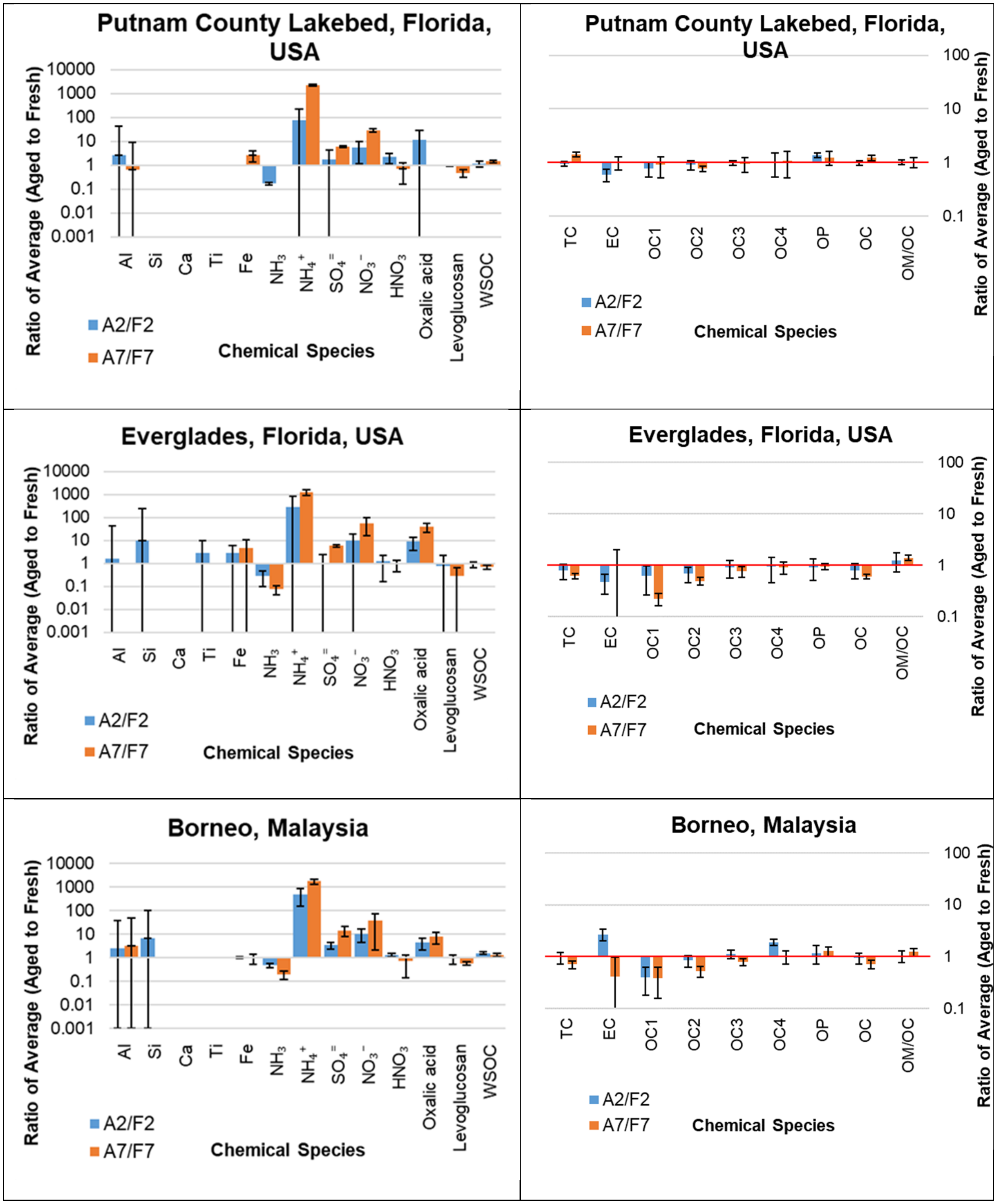

Figure 3. Ratios of average Aged (A) to Fresh (F) chemical species for 2-days (A2/F2) and 7-days (A7/F7) of atmospheric aging of six types of peats. Vertical bars represent the standard deviations associated with each ratio. Note that different scales were used in the two Y axes, with 0.001 to 10,000 on the left axis and 0.1 to 100 on the right axis (species abbreviations are shown in Fig. 1; OM is organic mass).

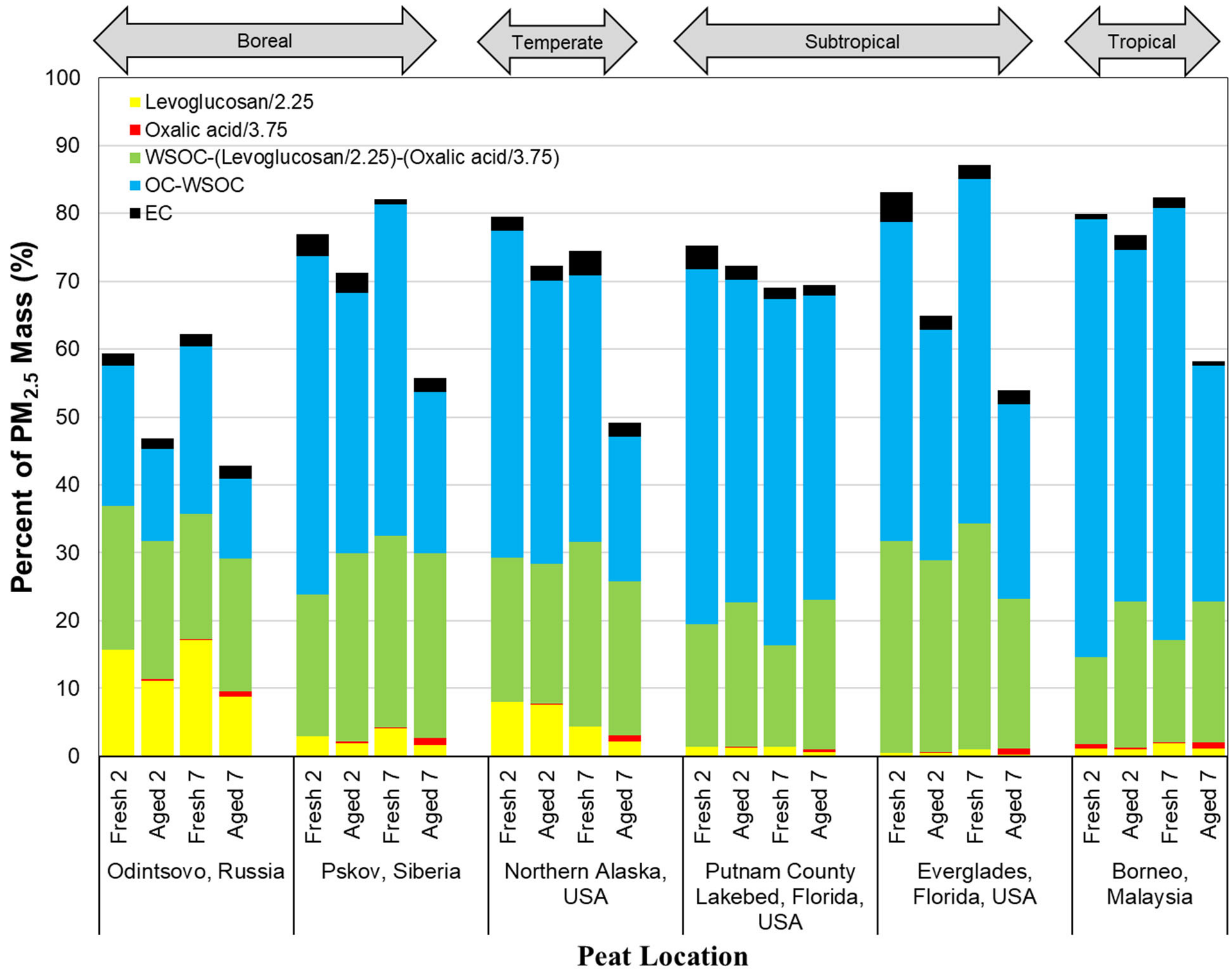

Figure 4. Abundances of fresh and aged carbon-containing components in $PM_{2.5}$ (levoglucosan [$C_6H_{10}O_5$] is divided by 2.25 and oxalic acid [$C_2H_2O_4$] is divided by 3.75 to obtain the carbon content. These levels are subtracted from the water-soluble organic carbon [WSOC] to obtain the remainder, and WSOC is subtracted from organic carbon [OC] to obtain non-soluble carbon. Elemental carbon [EC] is unaltered).

(a) NH_3 and NH_4^+

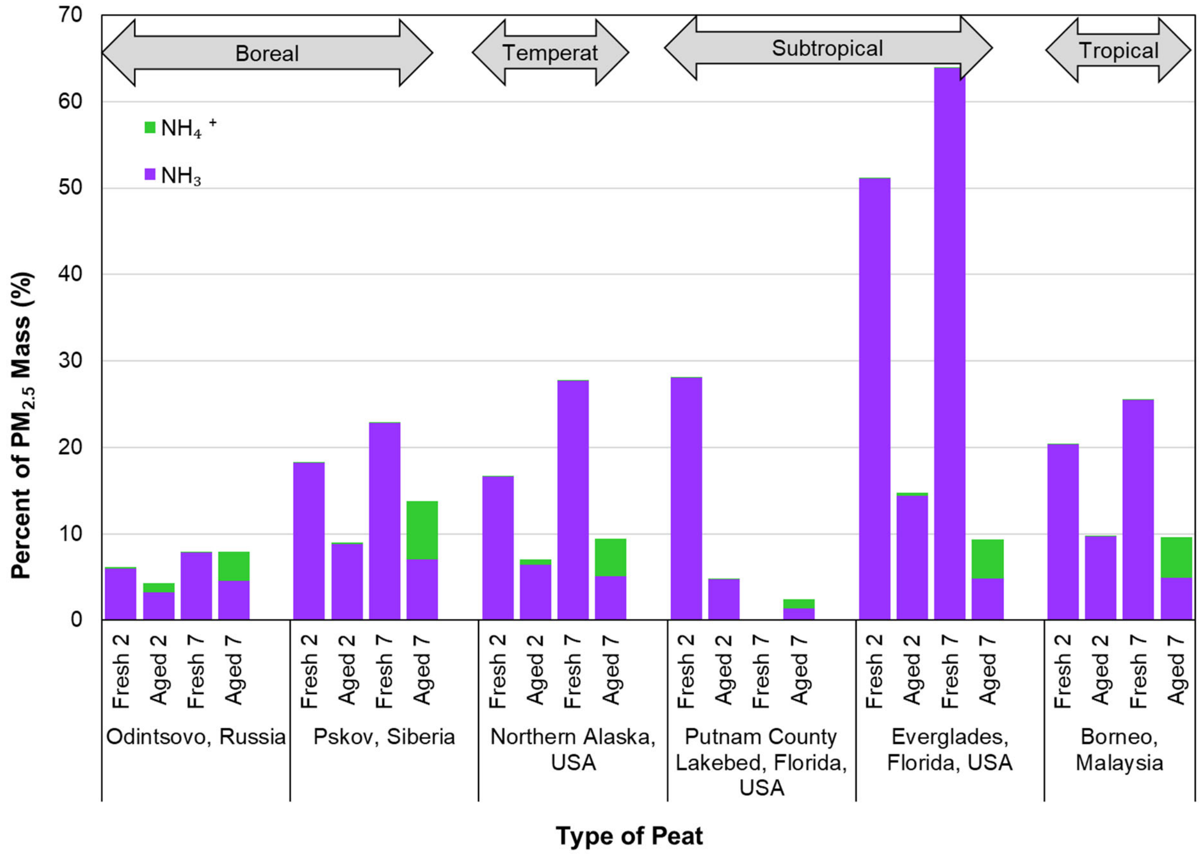

(b) HNO_3, NO_2^-, and NO_3^-

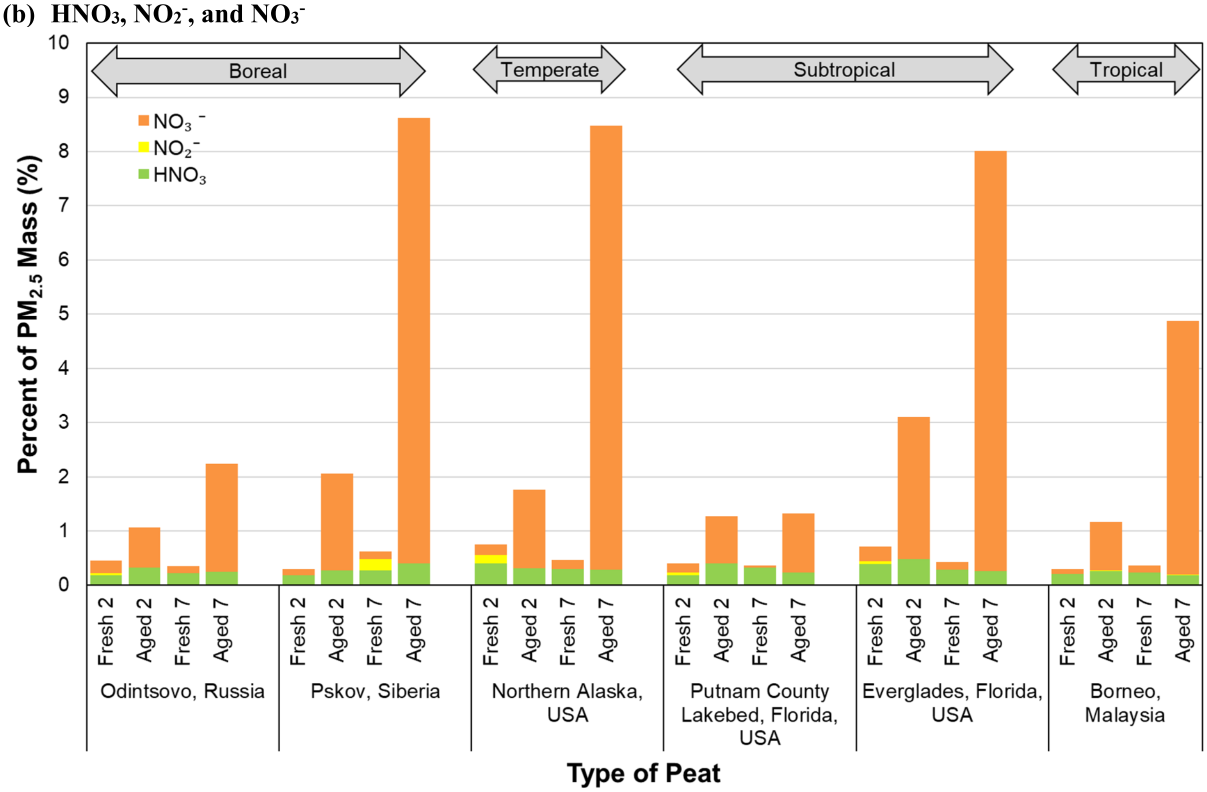

Figure 5. Comparison of nitrogen species for: a) NH_3 and NH_4^+; and b) HNO_3, NO_2^-, and NO_3^- between fresh and aged profiles for six types of peats.

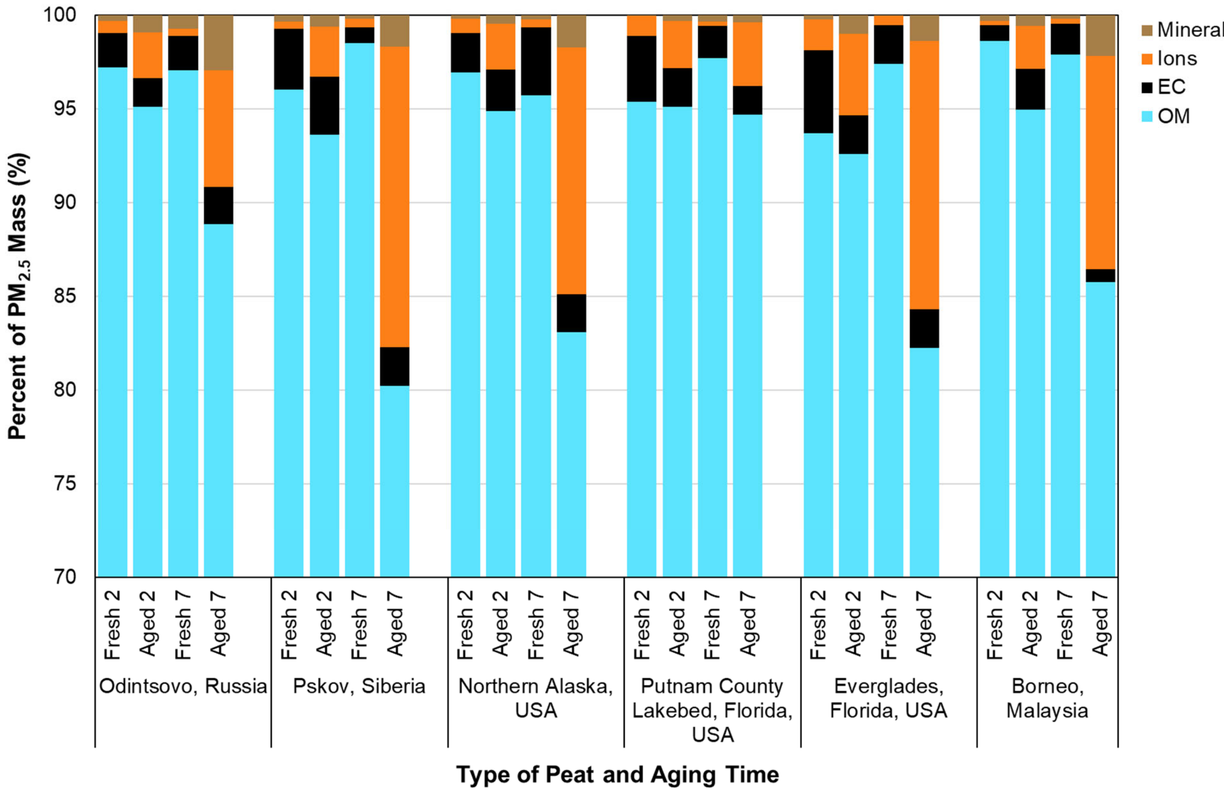

Figure 6. Reconstruction of $PM_{2.5}$ mass with organic mass (OM, see Table 3 for OM/OC ratios), elemental carbon (EC), major ions (i.e., sum of NH_4^+, NO_3^-, and $SO_4^{=}$), and mineral component (=2.2 Al + 2.49 Si + 1.63 Ca + 1.94 Ti + 2.42 Fe) for six types of peat between fresh and aged profiles.